Electrospinning of Fibres with Hydrophobic Surface

Bc. Aneta Cmarová

Master thesis
2017

Tomas Bata University in Zlín
Faculty of Technology

Univerzita Tomáše Bati ve Zlíně
Fakulta technologická
Ústav inženýrství polymerů
akademický rok: 2016/2017

ZADÁNÍ DIPLOMOVÉ PRÁCE
(PROJEKTU, UMĚLECKÉHO DÍLA, UMĚLECKÉHO VÝKONU)

Jméno a příjmení:	**Bc. Aneta Cmarová**
Osobní číslo:	**T15254**
Studijní program:	**N2808 Chemie a technologie materiálů**
Studijní obor:	**Inženýrství polymerů**
Forma studia:	**prezenční**
Téma práce:	**Příprava vláken s hydrofobním povrchem pomocí elektrostatického zvlákňování**

Zásady pro vypracování:

1. **Literární rešerše na sledované téma**
2. **Příprava polymerních roztoků**
3. **Elektrostatické zvlákňování a měření povrchových vlastností připravených vláken**
4. **Zpracování výsledků, jejich diskuze**

Rozsah diplomové práce:

Rozsah příloh:

Forma zpracování diplomové práce: **tištěná/elektronická**

Seznam odborné literatury:

1. RAMAKRISHNA, S., et al. An introduction to electrospinning and nanofibers. Singapore: World Scientific, 2005.
2. RENEKER, D. H.; et al. Nanometre diameter fibres of polymer, produced by electrospinning. Nanotechnology, 7(1996).p.216
3. XU, H.; at al. Controlled drug release from a polymer matrix by patterned electrospun nanofibers with controllable hydrophobicity. Journal of Materials Chemistry B, (2013), p.4182

Vedoucí diplomové práce: **Ing. Martin Stěnička, Ph.D.**
Ústav inženýrství polymerů

Datum zadání diplomové práce: **2. ledna 2017**

Termín odevzdání diplomové práce: **10. května 2017**

Ve Zlíně dne 1. března 2017

L.S.

UNIVERZITA TOMÁŠE BATI VE ZLÍNĚ
Fakulta technologická

doc. Ing. František Buňka, Ph.D.
děkan

doc. Ing. Tomáš Sedláček, Ph.D.
ředitel ústavu

Příjmení a jméno: ANETA CMAROVÁ Obor: CATM - IP

PROHLÁŠENÍ

Prohlašuji, že

- beru na vědomí, že odevzdáním diplomové/bakalářské práce souhlasím se zveřejněním své práce podle zákona č. 111/1998 Sb. o vysokých školách a o změně a doplnění dalších zákonů (zákon o vysokých školách), ve znění pozdějších právních předpisů, bez ohledu na výsledek obhajoby [1)];
- beru na vědomí, že diplomová/bakalářská práce bude uložena v elektronické podobě v univerzitním informačním systému dostupná k nahlédnutí, že jeden výtisk diplomové/bakalářské práce bude uložen na příslušném ústavu Fakulty technologické UTB ve Zlíně a jeden výtisk bude uložen u vedoucího práce;
- byl/a jsem seznámen/a s tím, že na moji diplomovou/bakalářskou práci se plně vztahuje zákon č. 121/2000 Sb. o právu autorském, o právech souvisejících s právem autorským a o změně některých zákonů (autorský zákon) ve znění pozdějších právních předpisů, zejm. § 35 odst. 3 [2)];
- beru na vědomí, že podle § 60 [3)] odst. 1 autorského zákona má UTB ve Zlíně právo na uzavření licenční smlouvy o užití školního díla v rozsahu § 12 odst. 4 autorského zákona;
- beru na vědomí, že podle § 60 [3)] odst. 2 a 3 mohu užít své dílo – diplomovou/bakalářskou práci nebo poskytnout licenci k jejímu využití jen s předchozím písemným souhlasem Univerzity Tomáše Bati ve Zlíně, která je oprávněna v takovém případě ode mne požadovat přiměřený příspěvek na úhradu nákladů, které byly Univerzitou Tomáše Bati ve Zlíně na vytvoření díla vynaloženy (až do jejich skutečné výše);
- beru na vědomí, že pokud bylo k vypracování diplomové/bakalářské práce využito softwaru poskytnutého Univerzitou Tomáše Bati ve Zlíně nebo jinými subjekty pouze ke studijním a výzkumným účelům (tedy pouze k nekomerčnímu využití), nelze výsledky diplomové/bakalářské práce využít ke komerčním účelům;
- beru na vědomí, že pokud je výstupem diplomové/bakalářské práce jakýkoliv softwarový produkt, považují se za součást práce rovněž i zdrojové kódy, popř. soubory, ze kterých se projekt skládá. Neodevzdání této součásti může být důvodem k neobhájení práce.

Ve Zlíně 5.5.2017 .....

[1)] *zákon č. 111/1998 Sb. o vysokých školách a o změně a doplnění dalších zákonů (zákon o vysokých školách), ve znění pozdějších právních předpisů, § 47 Zveřejňování závěrečných prací:*

(1) Vysoká škola nevýdělečně zveřejňuje disertační, diplomové, bakalářské a rigorózní práce, u kterých proběhla obhajoba, včetně posudků oponentů a výsledku obhajoby prostřednictvím databáze kvalifikačních prací, kterou spravuje. Způsob zveřejnění stanoví vnitřní předpis vysoké školy.

(2) Disertační, diplomové, bakalářské a rigorózní práce odevzdané uchazečem k obhajobě musí být též nejméně pět pracovních dnů před konáním obhajoby zveřejněny k nahlížení veřejnosti v místě určeném vnitřním předpisem vysoké školy nebo není-li tak určeno, v místě pracoviště vysoké školy, kde se má konat obhajoba práce. Každý si může ze zveřejněné práce pořizovat na své náklady výpisy, opisy nebo rozmnoženiny.

(3) Platí, že odevzdáním práce autor souhlasí se zveřejněním své práce podle tohoto zákona, bez ohledu na výsledek obhajoby.

[2)] *zákon č. 121/2000 Sb. o právu autorském, o právech souvisejících s právem autorským a o změně některých zákonů (autorský zákon) ve znění pozdějších právních předpisů, § 35 odst. 3:*

(3) Do práva autorského také nezasahuje škola nebo školské či vzdělávací zařízení, užije-li nikoli za účelem přímého nebo nepřímého hospodářského nebo obchodního prospěchu k výuce nebo k vlastní potřebě dílo vytvořené žákem nebo studentem ke splnění školních nebo studijních povinností vyplývajících z jeho právního vztahu ke škole nebo školskému či vzdělávacího zařízení (školní dílo).

[3)] zákon č. 121/2000 Sb. o právu autorském, o právech souvisejících s právem autorským a o změně některých zákonů (autorský zákon) ve znění pozdějších právních předpisů, § 60 Školní dílo:

(1) Škola nebo školské či vzdělávací zařízení mají za obvyklých podmínek právo na uzavření licenční smlouvy o užití školního díla (§ 35 odst. 3). Odpírá-li autor takového díla udělit svolení bez vážného důvodu, mohou se tyto osoby domáhat nahrazení chybějícího projevu jeho vůle u soudu. Ustanovení § 35 odst. 3 zůstává nedotčeno.

(2) Není-li sjednáno jinak, může autor školního díla své dílo užít či poskytnout jinému licenci, není-li to v rozporu s oprávněnými zájmy školy nebo školského či vzdělávacího zařízení.

(3) Škola nebo školské či vzdělávací zařízení jsou oprávněny požadovat, aby jim autor školního díla z výdělku jím dosaženého v souvislosti s užitím díla či poskytnutím licence podle odstavce 2 přiměřeně přispěl na úhradu nákladů, které na vytvoření díla vynaložily, a to podle okolností až do jejich skutečné výše; přitom se přihlédne k výši výdělku dosaženého školou nebo školským či vzdělávacím zařízením z užití školního díla podle odstavce 1.

ABSTRAKT

Vzájemný vztah mezi strukturou nanovlákenných vrstev připravených pomocí elektrostatického zvlákňování z roztoků polyvinylbutyralu a jejich snášivostí byl studován v rámci této práce. Polyvinylbutyral byl proto rozpuštěn v dobrém rozpouštědle (směs tetrahydrofuranu a dimetylsulfoxidu v objemových poměrech 9:1 a 8:2), tak i ve špatném rozpouštědle (metanol, etanol), protože to má výrazný vliv na konečnou strukturu vláken. Vedle toho byl sledován vliv rozdílné koncentrace polyvinylbutyralu v konkrétních rozpouštědlech a jejich ve směsích.

V prvním kroku byly připravené roztoky polyvinylbutyralu testovány různými metodami, a to pomocí elektrické vodivosti, měřením povrchového napětí a reologického chování. Následně byly zvlákňovány nanovlákenné vrstvy, které charakterizovány pomocí elektronové mikroskopie a měřením kontaktního úhlu.

Klíčová slova: elektrostatické zvlákňování • nanovlákna • polyvinylbutyral • hydrofobicita

ABSTRACT

A mutual correlation between the structure of electrospun fibrous layers prepared from polyvinylbutyral and their wettability was investigated within this study. Therefore, polyvinylbutyral was dissolved in a good solvent (mixtures of tetrahydrofuran and dimethylsulfoxide in volume ratios 9:1 and 8:2) and a poor solvent (methanol, ethanol), respectively due to the significant impact on the final structure of fibres. Besides, various concentrations of polyvinylbutyral in particular solvents and their mixtures were studied.

In the first step, polyvinylbutyral solutions were tested by means of various methods, namely electrical conductivity, surface tension and rheological behaviour was measured. Subsequently, nanofibrous layers were produced via electrospinning and characterized via scanning electron microscopy and contact angle measurements.

Keywords: Electrospinning • Nanofibres • Polyvinylbutyral • Hydrophobicity

ACKNOWLEDGEMENTS

Herein, it is my pleasure to thank those who made this thesis possible…

I would like to express my gratitude to my supervisor Martin Stěnička who provided me constructive comments and warm encouragement.

My grateful thanks belong to Petra Peer and Lenka Musilová who helped me with my experimental work. Their support and advices, whenever I needed, were inestimable.

Special thanks also to Institute of Hydrodynamic (Czech Academy of Science in Prague) and Institute of Physics and Material Engineering (Faculty of Technology in Zlín) for permission to perform some of my experiments.

I gratefully acknowledge to Institute of Materials Handling Technology and Plastics at Chemnitz University of Technology for creative environments during my traineeship.

I would also like to express my gratitude to Kuraray Europe, GmbH for their material support.

Last, but not least, I would like to express my gratitude to my family for their everlasting support, patience and understanding in course of my studying period.

.

I hereby declare that the print version of my Master's thesis and the electronic version of my thesis deposited in the IS/STAG system are identical.

CONTENT

INTRODUCTION

Electrospinning [1–3] is known as a simple and effective method for the production of nano- or rather microfibres from polymer solution or melt in the presence of static electric field. The first reference to preparation of the fibres in the static electric field is more than one century old. Nevertheless, there still exist some unanswered questions, which hinder a broader expansion. Perhaps, this is a reason, why the whole problematic permanently attracts the attention of both researchers and potential customers.

Electrospun fibres rank among the famous materials thanks to the high specific surface area which is guaranteed by very small diameter of fibres. Together with different morphologies (smooth, porous, flat, *etc.*) relatively easy reached by the controlling of material or processing parameters, the nanofibrous layers can be produced with various level of high porosity. This allows improving the surface wettability and further extending a portfolio of considered applications.

An inspiration can be found in the nature where surfaces with hydrophobic even more superhydrophobic behaviour commonly exist. A lotus leaf whose superhydrophobic surface is attributed to a combination of the nano- and microstructures on its surface can serve as a typical and well-known illustration.

Based on this fact, electrospinning seems to be a convenient technique for preparation of nanofibrous layers with controlled roughness on their surface, which provides them hydrophobic or even superhydrophobic behaviour.

I. THEORETICAL PART

1 ELECTROSPINNING

1.1 History of electrospinning

The electrospinning was firstly patented by Morton and Cooley in 1902 [4, 5]. In 1914, John Zeleny published a paper on the behaviour of fluid droplets at the end of metal capillaries. His effort began the attempt to mathematically model the behaviour of fluids under electrostatic forces. Nowadays, it is supposed that the real beginning of electrospinning started by Anton Formhals (1934) [6], who outlined an experimental setup for the production polymer fibres via electrostatic force as the first. His patent on electrospinning was issued for fabrication fibres from cellulose acetate using acetone and monomethyl ether of ethylene glycol as a solvent. Since this moment, an interest in utilizing this technique for production of nano- or microscale fibres with different structures from polymer solutions or melts accelerated, and resulted in a number of patents and publications [4–9]. For example, Simons (1966) [8] patented an apparatus for production of ultrathin, low weight and with different patterns non-woven fabrics by electrospinning. In 1971, Baumgarten [9] developed an apparatus to electrospin acrylic fibres with diameters in a range of 0.05 to 1.1 μm.

The process of electrospinning was intensively studied in the last decade of the previous century, what resulted in the development of the first needless electrospinning device, which allowed to postpone the process from laboratory work to the production in an industrial scale. New device was developed by Oldrich Jirsak et al. [10] in 2003 and patented under the commercial name Nanospider™. The principle of the device is shortly described in Subchapter 1.4.2.

1.2 Electrospinning process

Electrospinning is a relatively simple method in which nano- or rather microfibres in diameter are produced from polymer solutions or melts due to electrostatic forces.

During the process itself, the shape of the polymer solution droplet placed on the tip of the electrode changes after the application of a high electrical field between the tip and the collector. When a polymer solution is electrically charged enough, the droplet deforms from a semi-spherical shape (Figure 1a) into a conical structure called Taylor cone (Fig-

ure 1b). The charged polymer jet (Figure 1c) erupts from the droplet (from the Taylor cone on its surface, respectively) and accelerates toward the collector. The polymer jet can be split which contribute together with the high elongation rate to reduction of its diameter. And as a consequence of the rapid solvent evaporation, the jet lands as a solid fibre on the collector. [1–3]

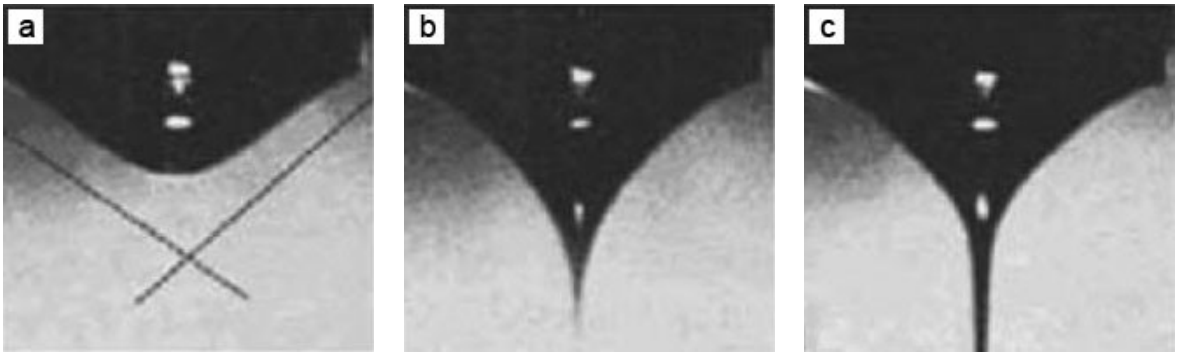

Figure 1 – An evolution process of the liquid drop and Taylor cone formation [11].

Basic characteristics of electrospinning are as follows:

- suitable polymer for fibre formation
- appropriate solvent for the chosen polymer
- optimal vapour pressure of the solvent
- proper viscosity and surface tension of the polymer solution
- adequate electrostatic field
- proportional distance between the electrode and grounded collector.

1.3 Influence of various parameters on electrospinning

Many recent studies [12–14] are focused on already well-known parameters participating in realisation and affecting the quality of electrospun fibres. They are usually divided into the four main groups as follows:

1. **polymer parameters** – molecular weight and molecular weight distribution, morphology of polymer (branched, linear, *etc.*),
2. **solvent parameters** – type of solvent (good or poor) and solvent volatility,

3. **solution parameters** – viscosity, concentration, conductivity, surface tension, dielectric constant of polymer solution,
4. **process parameters** – applied electric field, distance between electrode and collector, geometry of spinning and collecting electrode, and charge distribution, axial velocity, temperature, humidity and pressure. [1–3]

The most of critical parameters and their influence on process of fibres formation are discussed in the following Subchapters.

1.3.1 Polymer molecular weight

The molecular weight of polymer, which significantly effects many properties (viscosity, surface tension, conductivity and dielectric strength) ranks to the most discussed parameters. Generally known, a higher molecular weight increases the polymer resistance to solvent dissolution.

Reduction of beads and droplets as well as shape modification of fibres from circular to flat-like with increasing molecular weight was confirmed in Ref. [15]. Fibres were electrospun from polyvinylalcohol (PVA) aqueous solution, where PVA with various weight average molecular weight (M_w) was employed. The results show that fibre diameter increases and fibres without beads are observed with higher M_w.

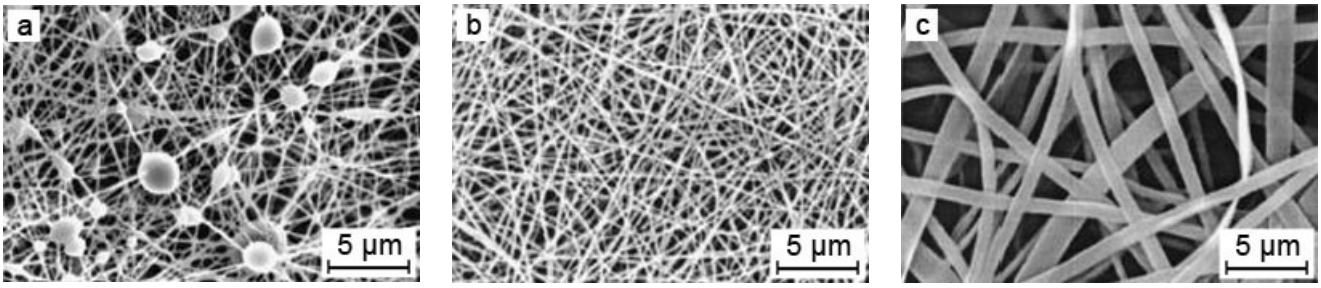

Figure 2 – Structure of electrospun fibres from PVA with various M_w: a) 9000 – 10 000 g/mol; b) 13 000 – 23 000 g/mol; and c) 31 000 – 50 000 g/mol [15].

1.3.2 Solvent properties

The electrospinning process requires a solvent to solubilise the polymer of interest. The correct selection of the solvent is a critical point to obtain a homogeneous solution of the polymer. The application of the solubility parameter is a practical way how to predict the polymer solubility or quality of the solvent. [16]

The Hansen solubility parameter (HSP, δ) [17] is accounted individually for all molecular interaction in polymer, such as dispersion forces, polar interactions (dipole-dipole), and specific interaction (hydrogen bonding). Then, the cohesive energy (eq. 1) is expressed as a sum of each contribution (eq. 2).

$$E = \Delta H - RT \tag{1}$$

where: E is the cohesion energy [J]; ΔH refers to the latent heat of vaporization [J]; R is the universal gas constant [$J \cdot K^{-1} \cdot mol^{-1}$]; and T is the absolute temperature [K].

$$E = E_D + E_P + E_H \tag{2}$$

Dividing E by the molar volume:

$$\frac{E}{V} = \frac{E_D}{V} + \frac{E_P}{V} + \frac{E_H}{V} \tag{3}$$

the HSP, δ [$MPa^{1/2}$] are obtained as a sum of three parts:

$$\delta^2 = \delta_d^2 + \delta_p^2 + \delta_h^2 \tag{4}$$

where: δ_d is the dispersive component [$MPa^{1/2}$], δ_p is the polar force component [$MPa^{1/2}$], and δ_h is the hydrogen bonding component [$MPa^{1/2}$]. These three parameters generate so called “Hansen space”. The nearer two molecules are in this space, the better they are able to be dissolved into each other, which is a criterion of a good solvent to a given polymer. The radius of the sphere, r (radius of interaction), indicates the maximum difference in affinity for which a good interaction takes place, see in Figure 3. [16, 18] HSP and r for commonly used polymers are calculated.

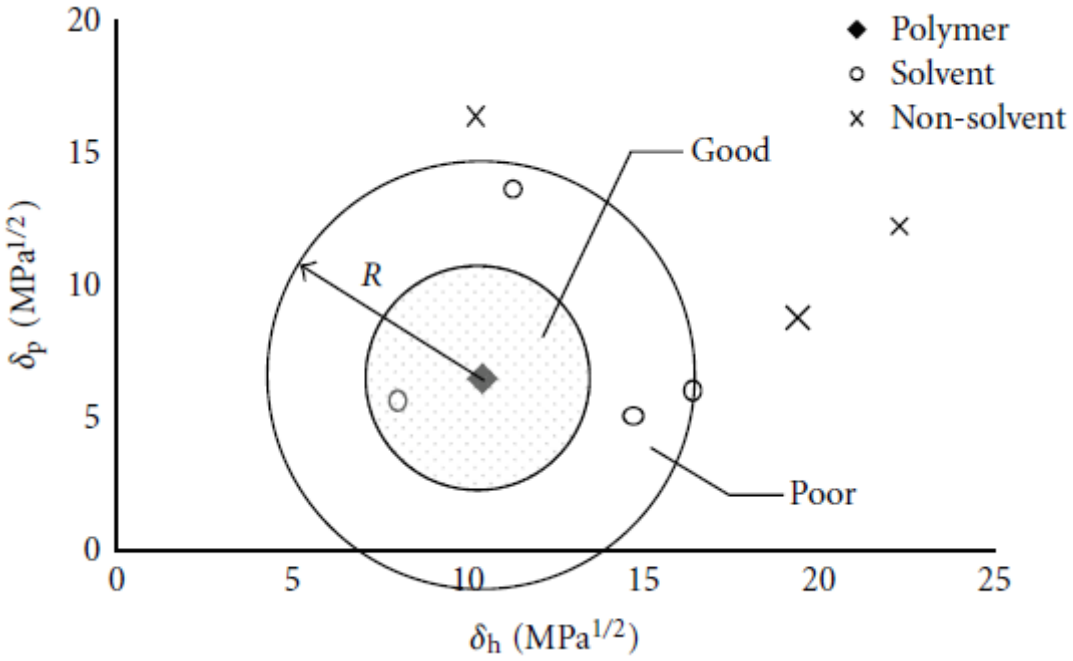

Figure 3 – Hansen 2D space of solubility area [19].

The influence of a good and a poor solvent is demonstrated, in Ref. [18]. PVB was dissolved in methanol (MetOH, poor solvent), and in isopropanol (good solvent). It was shown that PVB dissolved in MetOH exhibited better spinnability (smooth fibres without defects) than PVB in isopropanol. This was compared with their viscoelastic properties, where the solution containing poor solvent achieved higher elasticity in the presence of the electric field, and positively contributed to better electrospinnability.

1.3.3 Viscosity

Polymer solution viscosity plays an important role in the electrospinning process where determines the fibres size and morphology (uniform or beaded fibres). Generally, the viscosity is closely correlated to the amount of the entanglements of the polymer chains in a solvent. Therefore, polymer molecular weight, polymer molecular weight distribution and concentration of polymer in solution deeply affect the viscosity, see in Ref. [14, 20, 21].

When the viscosity is very low, discontinuous fibres are formed or electrospraying may occur. During the electrospraying, the polymer solution jet breaks up into the microdroplets, as seen in Figure 4a. On the other hand, when the viscosity is too high, it can be difficult to pump the polymer solution through the syringe needle, or the polymer solution

droplet at the tip of needle may dry out before the constant jet is formed as it was pointed out by Zong et al. [12]. Moreover, there can be a complication of jet eruption from polymer solution. [1]

Thus the optimal viscosity is necessary for successful electrostatic spinning. The range significantly varies for different polymers.

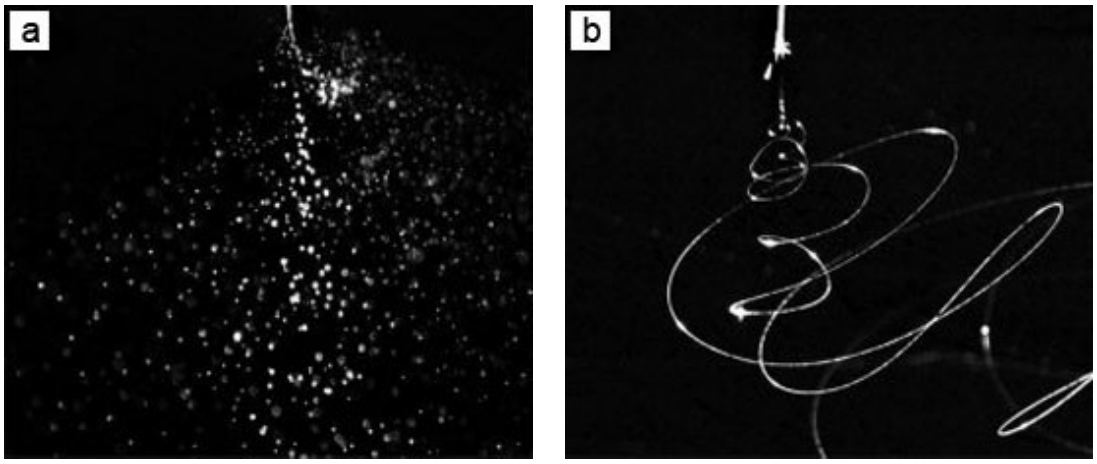

Figure 4 – Typical examples of a) electrospraying, and b) ideal electrospinning jet [22].

1.3.4 Concentration

Another factor, which has also an influence on the electrospinning process, is the polymer concentration. Usually, the diameter of fibres increases with higher polymer concentration, when other spinning conditions are kept constant. [23, 24] However, it was found a nonlinear relationship between the polymer solution concentration and fibres diameter, which can be attributed to the nonlinear relationship between the polymer concentration and viscosity of polymer solution [14].

Solution concentration has to be optimalized, otherwise fibres containing beads defects appear at low concentration. At too concentrated solutions, the formation of continuous fibres is prohibited due to the inability of the solution to flow at the needle top, or thicker fibres are produced. [25]

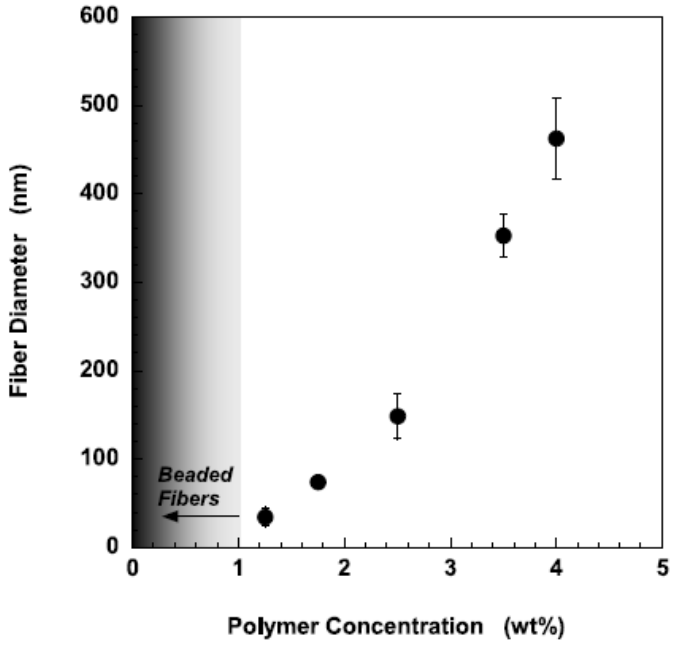

Figure 5 – The effect of polymer concentration on the diameter of electrospun poly-L-lactide (PLLA) (M_w: 300 K) fibres [13].

1.3.5 Polymer solution conductivity

Considerably higher conductivity given by addition of salts or drugs, or the increasing polarity of a solution results in the increase of the net charge density. Thus, the Coulombic repulsion and electrostatic forces increase, which cause the charged jet to be more stretched or extended and the fibres diameter is reduced. [7]

Lee et al. [26] studied the influence of solution properties of polycaprolactone (PCL) solutions prepared in three kinds of solvent system. In the first one, PCL was dissolved in methylene chloride (MC) only. In the second one, PCL was dissolved in a mixture of MC and *N*, *N*-dimethylformamide (DMF) in ratios of 100/0, 85/15, 75/25, and 40/60 (vol.%/vol.%). And finally, PCL was dissolved in a mixture of MC and toluene in ratios of 85/25 and 40/60 (vol.%/vol.%). MC, toluene and DMF are considered as a good, poor, and non-solvent for PCL, respectively. In Figure 6, the electric conductivity of MC/toluene systems is shown. The solution conductivity did not change as toluene content increased, whereas electrical conductivity of MC/DMF rises with higher DMF content. Similar effect was monitored for dielectric constant of solution dissolved in the mixture of MC/DMF, that was increased significantly when DMF added. It was found that both studied properties

had a significant effect on fibres morphology, mainly their diameter and the number of beads defects. Dielectric constant and solution conductivity strongly affected the diameter of electrospun fibres, where increasing DMF content ranging from 0 to 60 %. The average diameter of PCL fibres decreased from 5 500 to 200 nm.

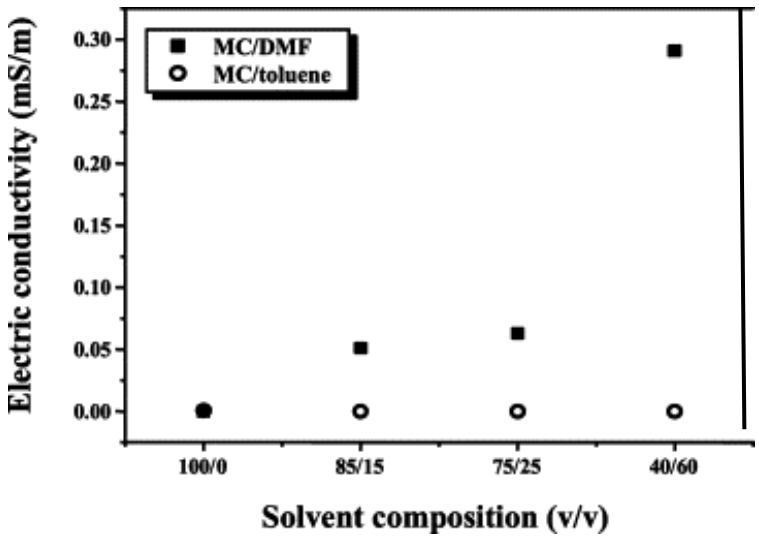

Figure 6 – The dependence of electric conductivity of PCL solution on solvent composition [26].

1.3.6 Surface tension coefficient

The surface tension coefficient is given by the type of a solvent, because various solvents contribute differently, and plays a critical role in electrospinning process. By reducing the surface tension (*e.g.* using different solvents or adding surfactants), beadless fibres can be produced. Moreover, polymer solutions with a lower surface tension can be spun at a lower electrical field, which allows to control fibre diameter. [1, 7]

Fong et al. [20] studied the influence of surface tension on fibres morphology. The solvent composition from neat water to water/ethanol (EtOH) mixture was continuously changed, whereas the polyethylene(oxide) (PEO) concentration was kept constant (Table I). Thus, smooth fibres with larger diameters were produced. It was found that the decreasing surface tension and the increasing viscosity of solution favours the formation of larger diameter fibres.

Table I – Composition and characteristic values of various PEO solutions [20].

Water [g]	EtOH [g]	Solution viscosity [10^{-3} Pa·s]	Solution surface tension [mN/m]
97	0	402	75.8
92	5	504	68.9
87	10	623	63.1
77	20	889	59.3
67	30	1129	54.7
57	40	1179	50.5

1.3.7 Applied voltage

Electrospinning process is initiated by the electric field, and therefore the intensity of applied voltage between electrode and the collector plays a fundamental role. The strength of the applied electric field can control formation of fibers and their diameter. Suboptimal field strength could lead to beads defects in the spun fibers or even to failure in jet formation. [27]

In my bachelor thesis [24], PEO aqueous solution (9 wt.%) was used to see the impact of intensity of electric field (ranging from 20 to 35 kV) on the quality of electrospun fibres. The results showed, that no fibres were produced at intensity of electric field under 20 kV. As the intensity of electric field increases, the fibres were gradually created, but their diameter was slightly reduced (Figure 7), and small beads defects appeared.

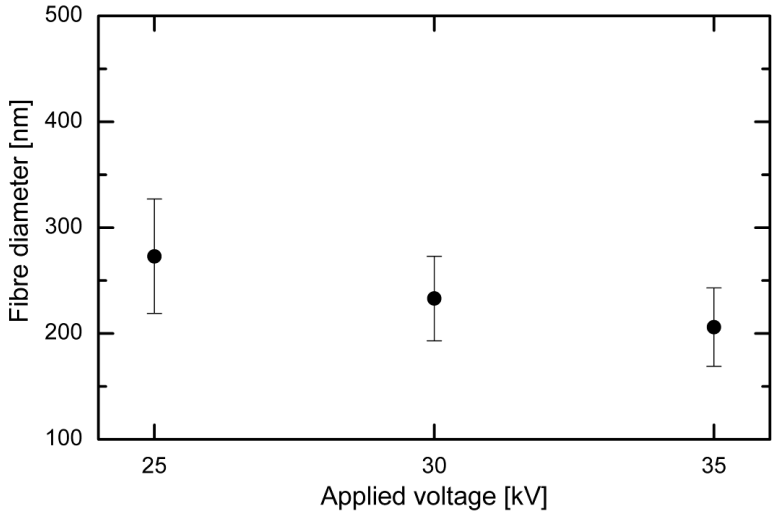

Figure 7 – Fibres diameter *vs.* intensity of employed electric field. The concentration of PEO in aqueous solution was 9 wt.% [24].

1.3.8 Influence of used electrospinning device

Differences in fibre morphology were also obtained when PVB solutions in different concentrations were spun by means of needle and roller technique. It was found out, that fibre diameters produced by needle electrospinning are smaller than these produced by roller electrospinning. Nevertheless, a closer view revealed that the single fibres are joined to bundles when produced. The higher throughput with increasing concentration leads to their sticking due to the higher density of fibres in the space between the electrode and collector. [23]

1.3.9 Effect of humidity

Humidity was found to directly affect the surface morphology of electrospun fibres. It was shown that electrospun fibres *e.g.* from polystyrene (PS) or polycarbonate (PC) contained submicron pores when the polymer was dissolved in a volatile solvent and electrospun under the humidity from 30 to 70 %. [7]

The changes of the fibre surface morphology were also demonstrated by Casper et al. [28]. The content of water in the air during the spinning from PS/tetrahydrofuran (THF) solution shows that smooth fibres were produced in the environment of humidity less than 25 %. Small pores were detected at humidity between 30 and 40 % (Table II and Figure 8). As

the humidity gradually increases the amount of circular pores grew up to the moment when the pores started to coalesce.

Table II – Diameter of PS/THF fibres under varying humidity levels [28].

Humidity range [%]	Range of pore diameters [nm]	Most frequent pore diameter [nm]
31 – 38	60 – 190	85
40 – 45	90 – 230	115
50 – 59	50 – 270	115
66 – 72	50 – 280	135

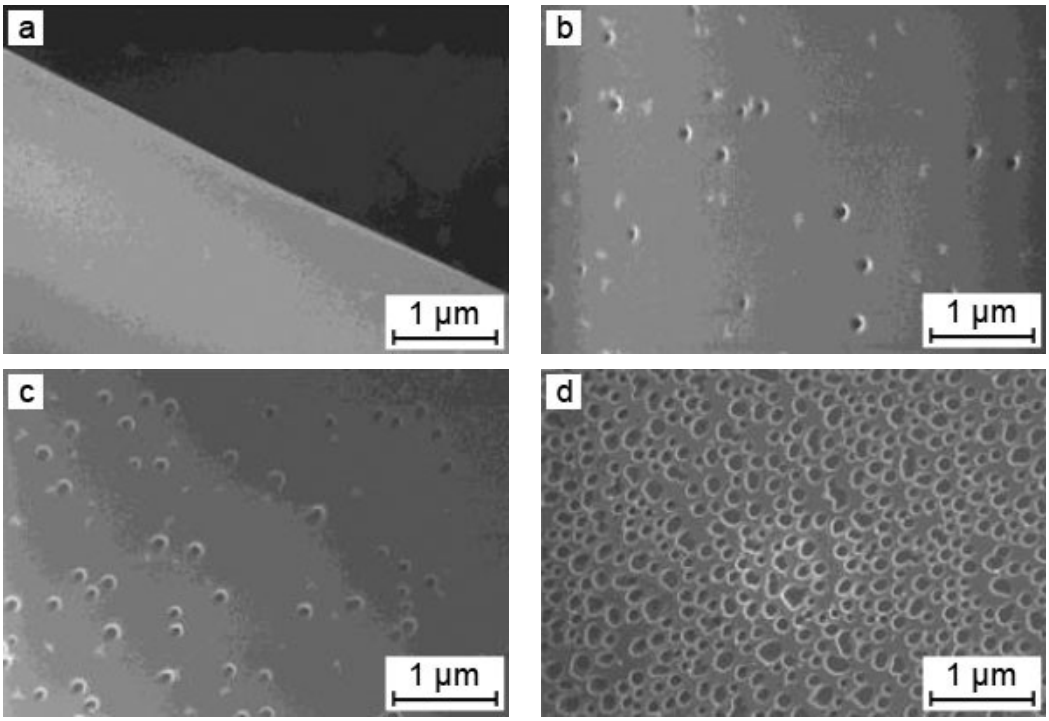

Figure 8 – Field emission SEM micrographs of 190,000 g/mol PS/THF fibres electrospun under varying humidity: a) < 25 %, b) 31 – 38 %, c) 40 – 45 %, and d) 50 – 59 % [28].

1.4 Principles of electrospinning devices

Electrospinning device is a relative easy equipment which consists of three main components: a DC high-voltage power supply, an electrode (needle, rod, roller, *etc.*), where

polymer solution is placed, and a grounded collector. Therefore, an enormous number of self-made laboratory devices were constructed. Two fundamental arrangements of electrospinning device are described and mutually compared in the next Subchapters.

1.4.1 Needle spinner

Needle spinner ranks to the simplest type of electrospinning device which is widely employed in laboratories due to the small amount of polymer solution needed. In principle, the solution is filled into a syringe and ejected from the needle. High voltage is applied when the solution leaves the needle tip. [2] Then the fibres are formed as it was described in Subchapter 1.2.

The fibre production is deeply influenced by the diameter of the needle and polymer solution flow rate. [1]

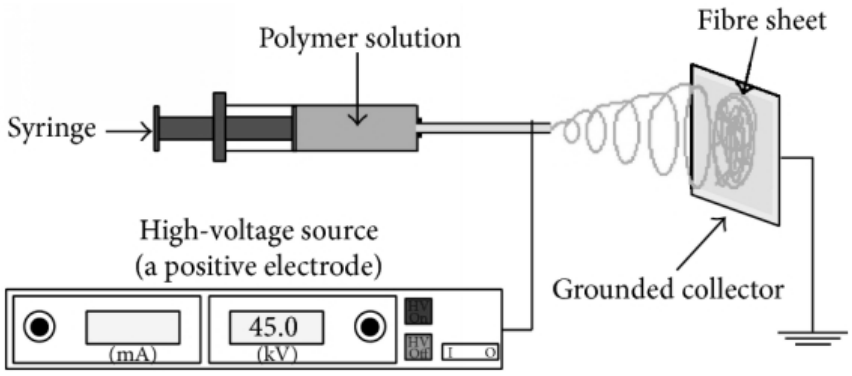

Figure 9 – A needle electrospinning system [29].

1.4.2 Needleless spinner

Needleless (*e.g.* rod, roller, wire) electrospinning methods are developed to prevent production problems such as needle clogging or low flow rate, which can occur by a needle spinner.

In the case of rod spinner, a droplet of polymer solution is placed on the rod electrode (Figure 10) and the fibres are spun directly from its free surface. The rod diameter plays an important role in the process of Taylor cones formation, because their number influences

the productivity. To obtain more than one Taylor cone, the rod with a diameter higher than 8 mm is usually used. [30] Nevertheless, this arrangement is suitable for laboratory work only due to the low production.

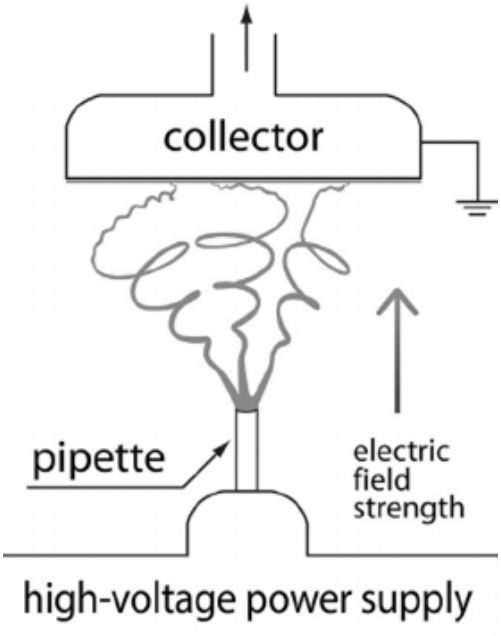

Figure 10 – A rod spinner [31].

Another type, which works on the principle of needleless electrospinning, uses a rotating roller as an electrode. The roller rotates with defined speed and is partially immersed in a tank containing electrospun solution (Figure 11). Thus, there is a layer of steadily fresh material on the surface of the roller, where many Taylor cones are created in the same time. This makes the electrospinning process highly productive in comparison to needle or rod electrospinning. [32] The principle was patented by Jirsak et al. and the produced device developed by Elmarco. Nanospider is considered mainly for production in industrial scale. [33]

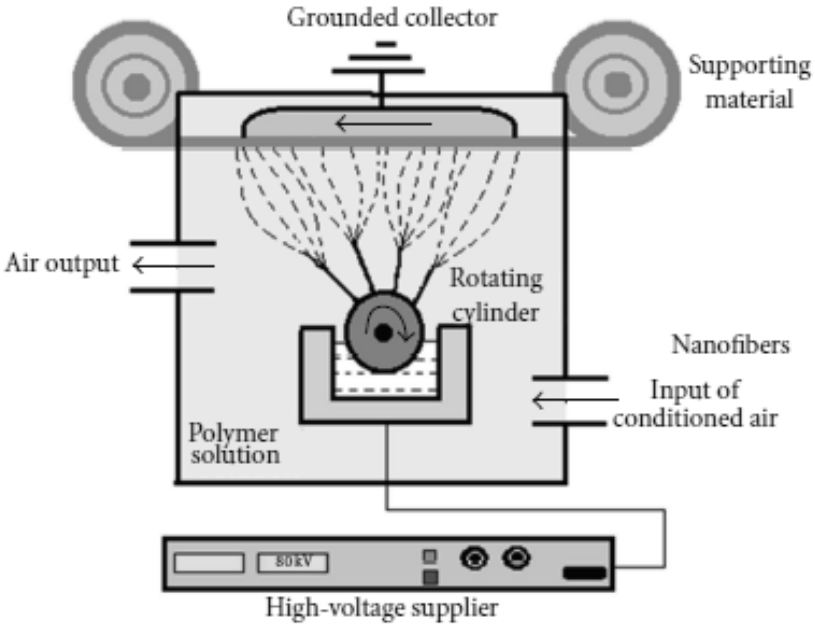

Figure 11 – A roller electrospinning system [23].

Figure 12 – Fibres spun from rotating cylinder [34].

1.5 Electrospun materials

By varying one or more parameters already discussed in Subchapter 1.3, fibres were successfully spun from different types of both, natural and synthetic polymers, polymer blends or polymer with additives (nanoparticle, drugs, *etc.*). A suitable material have to be selected in accordance to considered properties (biodegrability, non-toxicity, stability in various environment, *etc.*) and applications (filtration, tissue engineering, *etc.*).

Proteins (*e.g.* collagen [35, 36]), nucleic acid and polysaccharides (*e.g.* cellulose [37, 38]) representing natural polymers deserve a great attention. Among the synthetic polymers, PEO [24, 39, 40], polyacrylonitrile [41], polyvinylacetals (*e.g.* PVB [18, 19, 31]), polyamides [42, 43], PS [28, 44], polyurethanes [45–47], *etc.* were successfully electrospun in laboratory or in industrial conditions.

Bognitzki et al. [48] obtained copper nanofibres which were prepared by electrospinning of copper nitrate/PVB solution. After electrospinning, the thermal treatment firstly in air (conversion of copper nitrate to copper oxide and degradation of PVB) and later on in hydrogen atmosphere (conversion of copper oxide to copper) was applied. Thus, the inorganic materials, such as metal and ceramics [48], can be used for fibre preparation too, but the post-processing step (thermal treatment) of the electrospun fibres is required. Ultrafine electrospun fibres made from *e.g.* carbon [50], titanium dioxide [51] or copper oxide [52] produced in this way can be interesting for nanoelectronics, nanosensorics or nanofiltration. [48] This way of fibres production can be compared with technology of powder injection moulding.

1.6 Morphology and structure formation

In the recent years, polymer nanofibres gain attention as a promising material in many areas of application due to their unique properties as follows:

- high specific surface area,
- small pores diameter,
- high surface to weight ratio,
- high surface energy,
- good strength per unit weight,
- covering effects.

It would not be possible to guarantee this properties without the modification of the fibres morphology. Various morphology (beaded, porous, smooth, ribbon, core shell and hollow fibres) can be relatively easy achieved by changing electrospinning parameters. [53]

Certainly, the change of the morphology (smooth, beaded, and porous) also influences the wetting behaviour and specific adsorption ability of the spun fibres. However, not enough

research attention was paid to this topic so far. Therefore, it is a main object of aim in this study.

Smooth fibres

The morphology of electrospun fibres is usually circular and uniform with smooth surface (Figure 13). Such fibres are formed when the parameters (*e.g.* concentration or surface tension) are optimized for a given polymer solution. But, the production this type of fibres is complicated, since it is not easy to set up all parameters correctly.

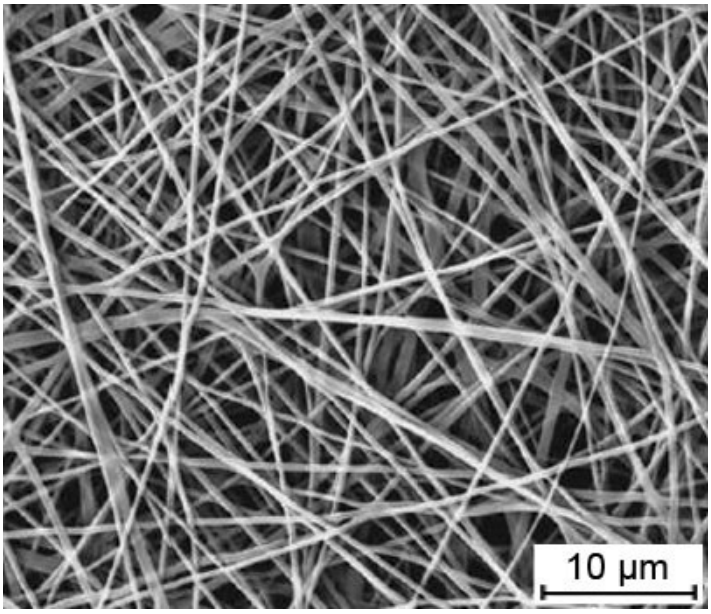

Figure 13 – Smooth PVA nanofibres [54].

Beaded fibres

Fibres prepared by electrospinning very often contain beads defects (Figure 14), which are caused especially by the solution properties. Generally, beaded fibres were considered as a undesirable defects of the final products. [55] However, extensive studies demonstrated that beaded fibres increase hydrophobic properties. Particularly porous, beaded fibres show strong hydrophobic properties, as published in Ref. [56].

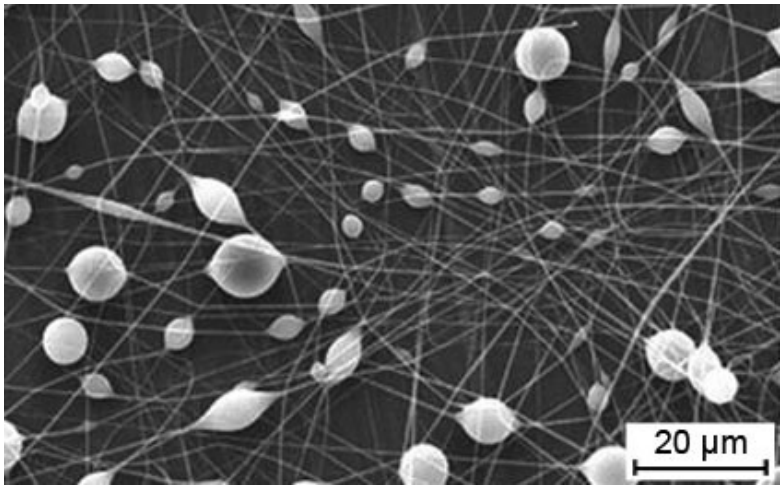

Figure 14 – Poly(methyl methacrylate) (PMMA) fibres electrospun from 20% PMMA/DMF solution [57].

Porous fibres

Fibres with porous morphologies can be prepared from multi-component solution via electrospinning under specific conditions (temperature, humidity), where one of this component is extracted during the production. But this method is technically difficult (two steps production). [19] There exists an easier way how to prepare porous fibres with various pore shapes (circular, oval) and pore size in one step process, when a combination of solvents is employed. Three necessary conditions to obtain the porous fibres are required: mixture of solvent/non-solvent for a given polymer, a difference of evaporation rate between solvent/non-solvent, and a suitable ratio of solvent/non-solvent in mixture. [19, 58]

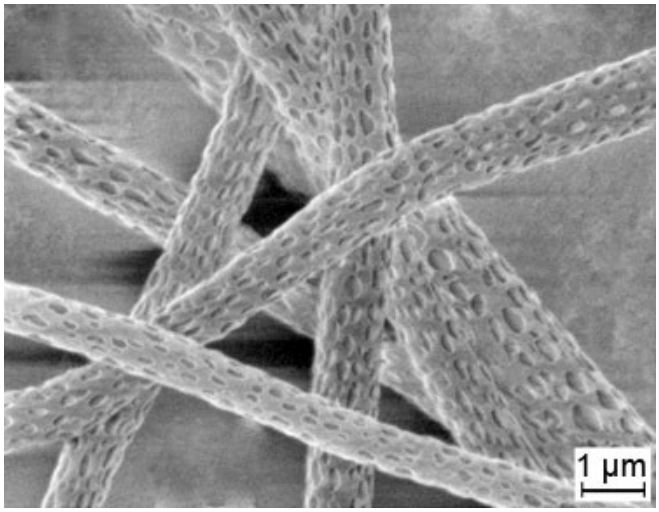

Figure 15 – Porous PLLA fibers obtained via electrospinning of a solution of PLLA in dichloromethane [53].

The use of volatile solvents, namely dichlormethane, ensures polymer fibres with a regular pore structure of PLLA fibres. It was explained that the regular phase morphology is generated by rapid phase separation during electrospinning process. The region rich for solvent is apparently transformed into the pores. [53]

1.7 Applications of electrospun fibres

Electrospun fibres, as a part of the nonwovens industry, were firstly commercialized for filter applications. Later on, the researches tried to expand into the new areas – wound healing, drug delivery, tissue engineering, protective clothing, or as sounds absorbing materials. [59]

1.7.1 Filtration

Filtration is a classical application field area, in which the air filters are already extensively used. Small fibre diameter corresponding to large specific surface area, small and controllable pore size, which are the basic characteristics of nanofibres, provide them excellent filtration properties. Very low weight of nanofibre layers, typical for nanofibre filter media, results in reasonably low values of pressure drop together with the high filtration efficiency. Besides, hydrophobic modification of filters is the most appropriate for gas filtra-

tion, low surface tension solvents, and venting. Water or aqueous solution can also pass through a hydrophobic filter once the water breakthrough pressure is reached.

Jirsak et al. [32] studied filtration efficiency of a viscose filter covered with very light nanofibre layers (0.03 – 0.1) g/m^2 and the results are shown in Figure 16. The nanofibres with diameter of 100 and 200 nm were used. The results show a considerable increase in filtration efficiency when nanofibre layers are combined with a standard filter material.

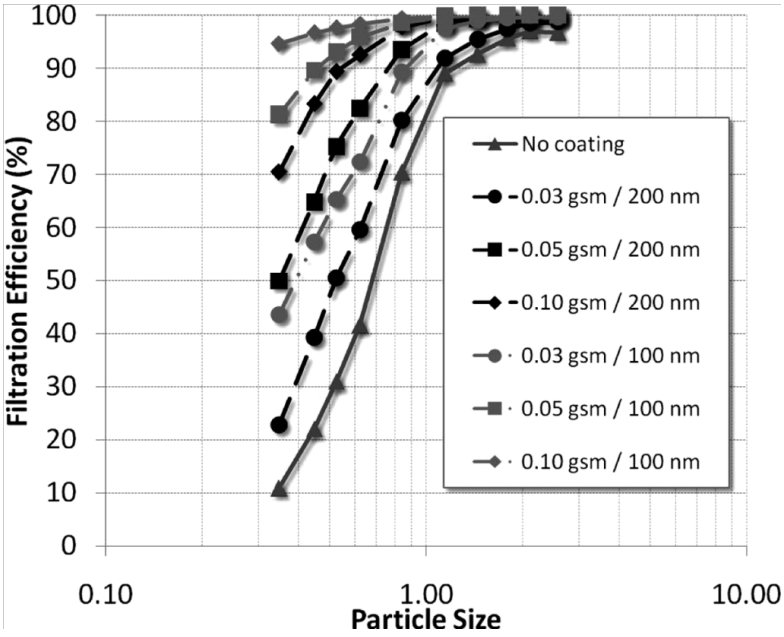

Figure 16 – Dependence of filtration efficiency (%) of nanofibre layers on particle size (μm) [32].

1.7.2 Sounds absorbers

Apart from filtration, the problematic of low-frequency sounds absorption can be solved with fibrous materials made up of coarser fibres. Therefore, these highly efficient sound absorbing materials were developed. The porosity, density of the fibre and the fibres fineness, have an important role, because one of the most important criteria of sounds absorbers are their structural characteristics.

The results from Kalinova [60] showed that standard soundproofing materials are effective in sounds absorbing at frequencies above 2 000 Hz only, whereas the materials containing nanofibre layers can absorb sound already at frequencies around 600 Hz.

1.7.3 Barrier textiles

Water repellency and self-cleaning properties typical for hydrophobic fibrous materials attract big attention recently. Barrier textiles containing hydrophobic nanofibre layers, *e.g.* polyurethane, PVB, or polyvinylidene fluoride, are an effective barriers for microorganism penetration (viruses, bacteria, molds), or for hazardous solid particles. Barrier textiles are normally produced in sandwich structure, where the nanofibre layer is enclosed between two layers (carrier and covering layer). The sandwich structure is produced by laminating the covering layer to the carrier layer. Such barrier textiles are usable for surgical drapes or in disposable breathing apparatus. [61]

2 HYDROPHOBICITY

The wetting behaviour of a liquid on a solid surface is a very crucial aspect of surface properties which plays an important role in industry and daily life. Hydrophobic surface attracted rapidly growing interest by discovery of "lotus effect" originated from mimicking the lotus leaves, which causes water and even oils to roll off with no or little residue left in all directions. In contrast to lotus leaves, the surfaces of rice, bamboo, and some grass leaves behave anisotropically. This means that water droplets can roll off in the prefered directions only. It was found that the special wettability correspondents to the unique micro- and nanostructures of surface rather than an intrinsic material property (*e.g.* rough surface of the lotus leaf, Figure 17a, b). Learning from the nature gave an inspiration to construct roughened and patterned solid surfaces, which are highly desired for new techniques (*e.g.* self-cleaning and antifouling properties) due to their special wettability. A popular method how to prepare the patterned surface with controlled wettability by constructing specific micro- and nanostructure on surface is electrospinning. Electrospun fibrous layers usually have high surface roughness, and therefore seems to be an ideal candidate for construction of hydrophobic surfaces on a large scale (Figure 17c, d). [55, 62, 63]

2.1 Characterization of surface wettability

To be more specific, hydrophobicity and hydrophilicity are qualitative terms that describe the surface interaction with water. Hydrophobic surfaces generally repel water and tend to absorb no water, mix with it or adsorb it, whereas the hydrophilic surfaces present the opposite behaviour. [66]

Several methods (contact angle measurement, tilt angle, or multiresonance thickness-shear mode sensor) were developed to characterize water repellency of the surface [67]. Among them, the contact angle measurement is the most frequently used method for characterization of the surface energy. There are three possibilities of wetting behaviour. When the contact angle (θ) is:

1. $\theta = 0°$ the surface is complete wetted,
2. $0° < \theta < 90°$ the surface is defined as hydrophilic,
3. $90° \leq \theta < 180°$ the surface is defined as hydrophobic.

The surface with water contact angle close to or higher than 150° is rather termed as super-hydrophobic. [62, 67]

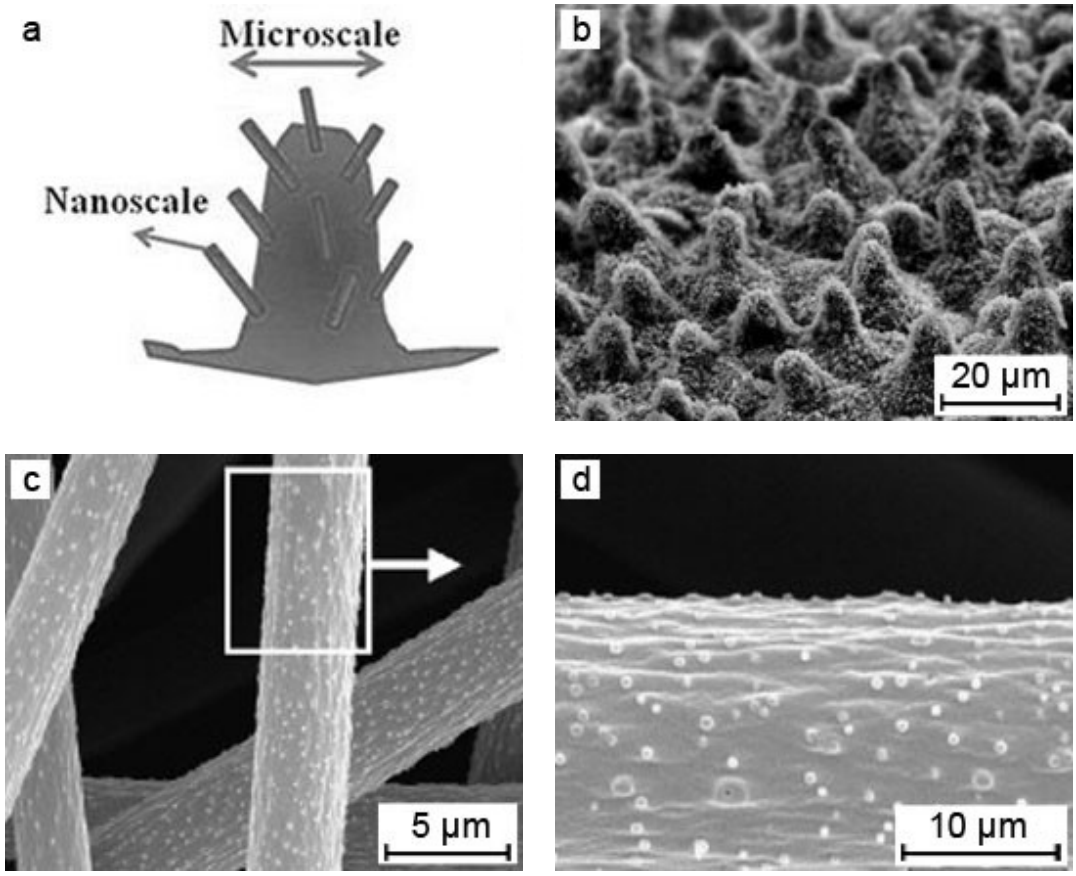

Figure 17 – a) Micro- and nanostructure of a single micropapilla presented on the surface of the lotus leaf [63], b) SEM image of the surface structure on the lotus leaf [55], c) and d) SEM image of the electrospun PS fibres from 35 wt.% solution in DMF [65].

2.1.1 Contact angle measurement

Contact angle measurements can be related to surface tensions or energies via Young´s equation (eq. 5), which takes into an account the surface energies of the involved interfaces. These surface energies come from the solid, liquid and solid/liquid interfaces. [64]

$$\gamma_{SG} = \gamma_{SL} + \gamma_{LG}.\cos\theta \tag{5}$$

where: γ_{SG} is the interfacial tension between the solid and gas [mN/m]; γ_{SL} is the interfacial tension between the solid and liquid [mN/m]; γ_{LG} is the interfacial tension between the liquid and gas [mN/m], and θ is the angle formed by a liquid at the three-phase boundary where the liquid, gas, and solid intersect, Figure 18.

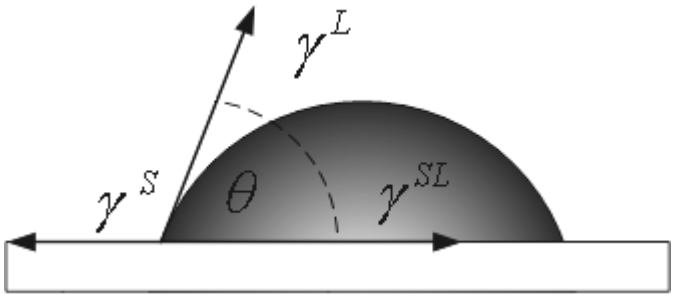

Figure 18 – The contact angle and interface energy between three phases [68].

3 POLYVINYL BUTYRAL

PVB belongs to a thermoplastic polymers, namely to the polyvinylacetals. PVB is amorphous random copolymer produced by the condensation of PVA with butyraldehyde in the presence of an acid catalyst. [69–71] It is the most important polyvinylacetal which participate 90 % of the worldwide production of polyvinylacetals [72].

3.1 Preparation of polyvinylbutyral

Synthesis of PVB is not easy. At first, polyvinyl acetate (PVAC) has to be produced by radical emulsion or suspension polymerization. After that, PVA is obtained by the direct hydrolysis (or catalyzed alcoholysis) of PVAC. PVA, as a precursor, provides PVB by acetalization with butyraldehyde at acid environment. [73]

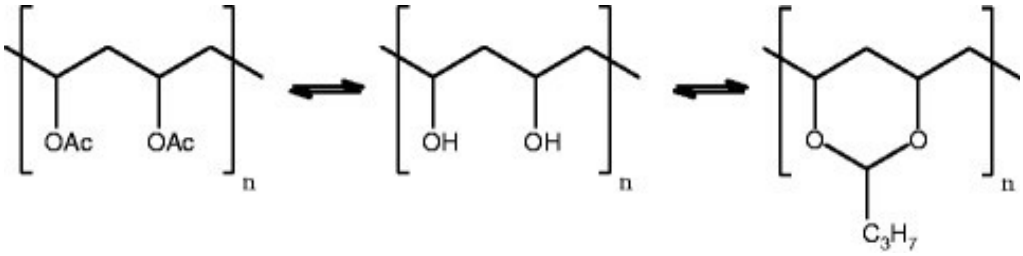

polyvinyl acetate polyvinyl alcohol polyvinyl butyral

Figure 19 – Synthesis of PVB preparation [74].

Since PVA is produced from the hydrolysis of PVAC, there is a limited amount of acetate groups also present. The structure of PVB consists of:

- acetal (butyral) groups (PVB): 70 – 82 %
- hydroxyl groups (PVA): 13 – 25 %
- acetate groups (PVAC): 0 – 3 %. [75, 76]

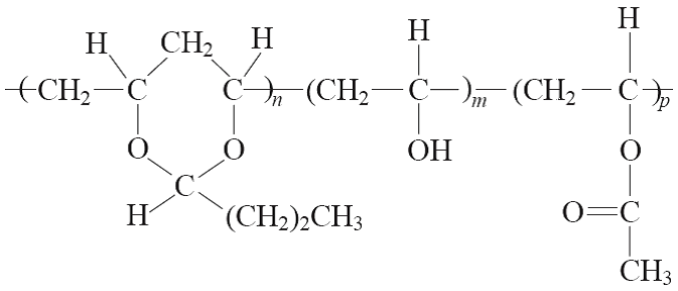

Figure 20 – Structural formula of PVB [77].

3.2 Physical and chemical properties

The final PVB properties are assigned by polymerization degree of PVAC, distribution curve of molecular weight, PVA hydrolysis degree, catalyst acid strength, reaction temperature and PVA conversion degree to PVB. [74]

The chemical composition of PVB is very important because it dramatically influences the properties of the polymer. The vinyl butyral unit is hydrophobic and promotes good processibility, toughness, elasticity and compatibility with many polymers and plasticizers. The hydrophilic vinyl alcohol and vinyl acetate units are responsible for high adhesion to inorganic materials such as glass or metal. [74]

The PVB polymer is a nontoxic, odourless, white powder, dissolvable in a large number of organic solvents (*e.g.* ethanol, THF, ketones and other polar solvents). The PVB solubility depends on the -OH group content in the polymer chain, whereas molecular weight has a secondary effect. In order to improve chemical, thermal and solvent resistance, PVB can be cross-linked due to the presence of –OH groups. Phenolic, melamine, epoxy, isocyanate, aldehyde and formaldehyde hydrate can be used. [70, 74]

M_w of the most industrial PVBs ranges of 40 000 – 250 000 g/mol. The density of PVB varies from 1.083 to 1.100 g/cm^3 according to vinyl alcohol content (11 – 19 wt.%). [74]

The glass transition temperature declines as the number of butyral groups increases and the polymerisation degree decreases. Values between 63 and 84 °C are measured for the various types [78].

3.3 Applications

The most important application of PVB is a production of films for lamination of safety glass in automotive and architecture. It is given by the PVB film properties including toughness, good light resistance, excellent transparency and adhesion to glass.

Furthermore, low viscous PVB is used as binders, *e.g.* in printing inks, anticorrosive primers, plastic and wood lacquers, packaging lacquers and pigment preparations. PVBs are also used as temporary binders for ceramics since they burn without residue at temperatures above 500 °C. [78]

4 METHODS AND MATERIALS

All methods employed for characterization of PVB solutions, nanofibrous layers and basic introduction of the used solvents are briefly discussed in this Chapter.

4.1 Electrical conductivity

The electrical conductivity (also known as specific conductance) reflects the capacity of solution conduct an electrical current. Conductivity measurement is strongly affected by temperature. Thus, the sample temperature has to be monitored together with the conductivity. [79]

Electrical conductivity (κ) is the reciprocal of the electrical resistivity (ρ_s). It is described by the equation 6:

$$\kappa = \frac{1}{\rho_s} = \frac{l}{R_e A} \tag{6}$$

where: κ is the specific conductance [S/m], ρ_s is the specific resistivity [Ω·m], l is the distance between the electrodes [m], R_e is resistance [Ω], and A is cross-section area [m^2].

4.2 Surface tension measurement

4.2.1 Wilhelmy plate method

This method is used for measuring surface tension of a liquid, the interfacial tension between two liquids and the contact angle between liquid and solid. Wilhelmy plate method is based on measuring the instantaneous force acting on a vertically immersed platinum plate, see in Figure 21. To measure the force, the plate is attached to a force sensor of a tensiometer. The required variable surface tension (γ) is calculated according to equation 7:

$$\gamma = \frac{F}{L \cdot cos\theta} \tag{7}$$

where: γ is the surface tension [mN/m], L is the wetted length [m], and θ is the contact angle [°]. [80]

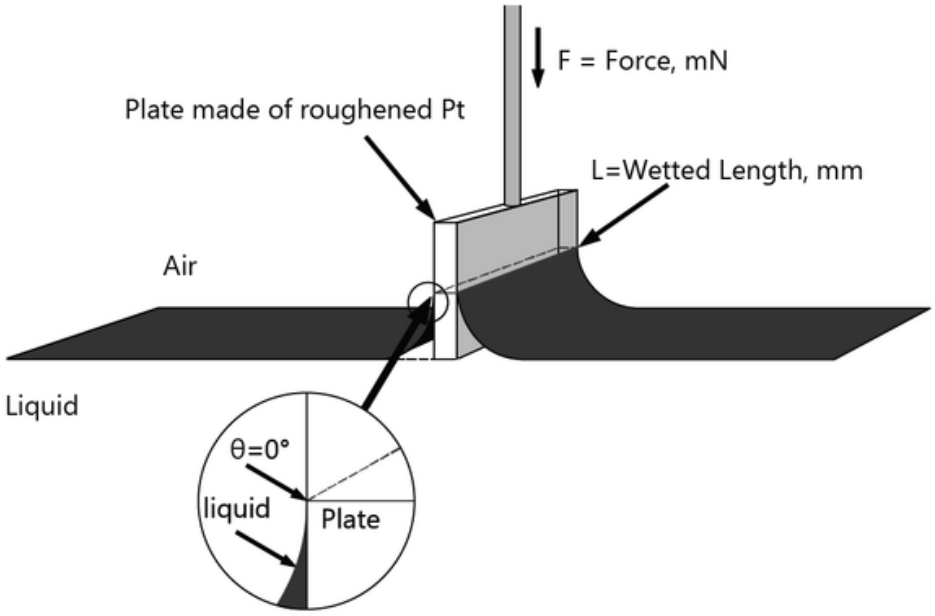

Figure 21 – Wilhelmy plate method [80].

4.2.2 Sessile drop method

Sessile drop method is usually measured with a goniometer. This method is based on placing a testing liquid (water, diiodomethane, *etc.*) onto the surface and spreading water on a surface by means of contact angle as depicted in Figure 22. The measurement of the spreading water onto surface represents the water adhesion tension, which estimates the wettability of a surface. Change in tension due to molecular interaction cause change in contact angle in three phase system: solid, liquid, and gas interface. This method is easy and can be effectively used for determination the hydrophobic character of prepared nanofibrous webs. [80]

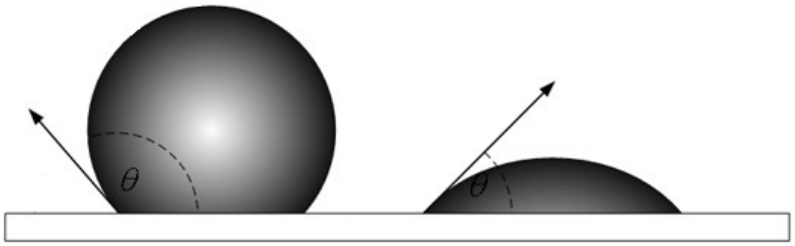

Figure 22 – The diagram of contact angle [68].

4.3 Rheological measurement

Rheology describes the deformation of solid and flow of liquid materials under the stress. The dynamic viscosity (η), a fundamental rheological parameter is defined as a ratio of the force (σ – stress) to the deformation rate ($\dot{\gamma}$ – shear rate).

$$\eta = \frac{\sigma}{\dot{\gamma}} \tag{8}$$

where: η is the dynamic viscosity [Pa·s]; σ is the shear stress [Pa]; and $\dot{\gamma}$ is the shear rate [s^{-1}].

Rheological behaviour can be measured by a variety of methods, including simple capillary viscometers, extrusion rheometers and rotational rheometers.

The rotational rheometers measure the stress at a known shear rate or measure the shear rate at a known stress to obtain the viscosity. These rheometers for evaluation of rheological properties of polymer solutions and polymer melts are equipped with cone-plate, parallel-plate and concentric cylinders (Figure 23). In the most cases, the upper part of the geometry is rotational moved, whereas a lower part is fixed.

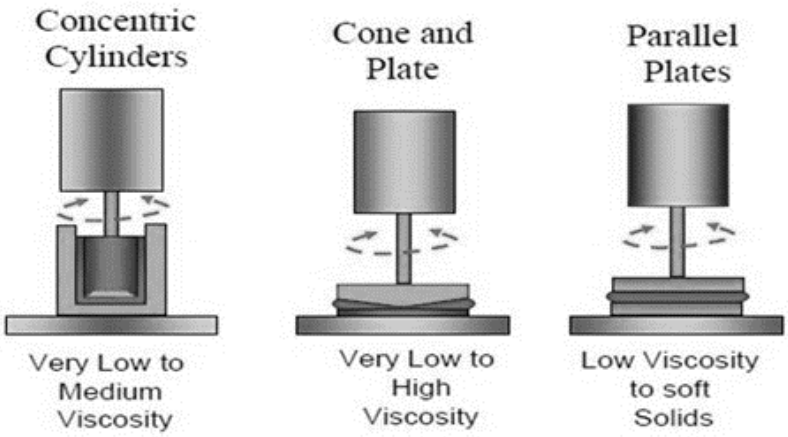

Figure 23 – Various geometries of rotational rheometer [82].

4.4 Scanning electron microscopy

Scanning electron microscope (SEM) is a powerful tool to obtain two dimensional image of the surface with a higher magnification and resolution than in light microscope since the wavelength of the electron (2×10^{-12} m) is much more smaller than wavelength of the visible light ($4 - 7 \times 10^{-7}$ m). Thus, the advantage of SEM microscopy is high magnification (up to 2,000,000×) and high resolution (up to 0.5 nm). SEM is widely used to investigate the morphology, chemical composition and crystalline structure of thin films or fibres and another nanostructures. [83] The scheme of SEM is shown in Figure 24.

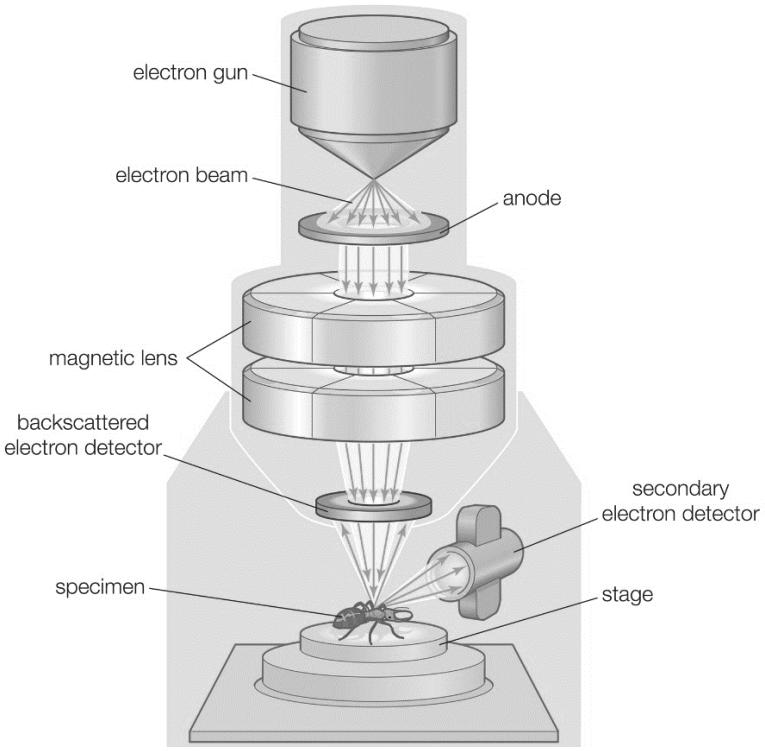

Figure 24 – Scanning electron microscope [83].

4.5 Solvents

In this part the used solvents are introduced shortly.

Methanol – is the simplest alcohol. It is a volatile, colourless, flammable and highly toxic liquid, which is used as a solvent, an antifreezing agent and as a denaturant for EtOH.

Figure 25 – Structural formula of MetOH.

Ethanol – is the most important type of alcohol. It is a volatile, flammable, colourless liquid with a slight characteristic odour. EtOH is widely used as a solvent, a fuel, and a basic substance for synthesis of other chemicals.

Figure 26 – Structural formula of EtOH.

Tetrahydrofuran – is an organic heterocyclic substance with strong ether-like odour. THF is a colourless, versatile solvent, miscible with water. It is mainly used as a precursor to polymers.

Figure 27 – Structural formula of THF.

Dimethylsulfoxide (DMSO) – This organosulfur substance is a colourless liquid which is an important polar solvent that dissolves both polar and non-polar compounds. It is miscible in a wide range of organic solvents as well as water.

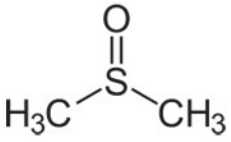

Figure 28 – Structural formula of DMSO.

Based on the literature review [19], the predicted morphology of electrospun fibres from PVB solutions in employed solvents are summarized in Table III.

Table III – Predicted morphology of prepared PVB fibres.

Solvent and solvent mixtures	**Morphology of nanofibres**
THF:DMSO (8:2)	porous
THF:DMSO (9:1)	porous
MetOH	nonporous
EtOH	nonporous

II. EXPERIMENTAL PART

5 POLYMER SOLUTIONS

5.1 Solutions preparation

Commercially available PVB Mowital B60H (Kuraray Europe, GmbH) with M_w = 60,000 g/mol was chosen for polymer solutions preparation. The structure of Mowital B60H is composed of vinyl butyral, vinyl alcohol and vinyl acetate (75 – 81 %, 18 –21 %, and 1 – 4 %).

For solution, PVB was dissolved in various solvents, namely EtOH (99% Brenntag GmbH, Germany), MetOH (99.5% Brenntag GmbH, Germany), and in two mixtures of solvents – THF:DMSO in volume ratios 9:1 and 8:2 (THF - 99% BASF Ludwigshafen, Germany; DMSO - 99% Grüssing GmbH, Germany). The polymer concentration in solvents was fixed at 6, 8 and 10 wt.%, respectively (Tables IV and V). All solutions were magnetically stirred (Rotilabo® MH 20, Carl ROTH, Germany) at 250 rpm at 20 ± 1 °C for 48 hrs.

Table IV – Composition of PVB solutions.

Concentration of solution	PVB [g]	MetOH; EtOH [g]	THF:DMSO (8:2); (9:1) [g]
6 wt.%	3	47	47
8 wt.%	4	46	46
10 wt.%	5	45	45

Table V – Basic characteristics of the solvents and PVB.

Polymer/ solvent	Specific conductivity [μS/cm]	Surface tension [mN/m]	Viscosity [mPa.s]	Boiling point [°C]	Hansen solubility parameters [$MPa^{1/2}$]			Character of solvent to PVB
					δ_d	δ_p	δ_h	
THF	4.5×10^{1}	26.40	0.460	66.0	16.8	5.7	8.0	good
DMSO	2.0×10^{-3}	42.90	1.996	189.0	9.0	8.0	5.0	poor
MetOH	1.5×10^{-3}	22.70	0.545	64.7	15.1	12.3	22.3	poor
EtOH	1.4×10^{-3}	22.39	1.078	78.3	15.8	8.8	19.3	poor
PVB	1.0×10^{-5}	-	-	-	18.6	4.4	13.0	-

For the purpose of solubility evaluation within this study, the HSP space was simplified to the 2D, where the δ_p and δ_h were taken into account only. With the respect to this, the employed solvents were arranged in the following sequence (good → poor): THF:DMSO (9:1) → THF:DMSO (8:2) → EtOH → MetOH.

5.2 Solutions characterization

Before the electrospinning process, the solution properties such as specific electrical conductivity, surface tension and shear viscosity were determined.

5.2.1 Electrical conductivity measurement

The electrical conductivity of all solutions was measured by means of Digital Conductometer CG 855 (SCHOTT Instruments, Germany). This conductometer was equipped with platinum electrode. Simultaneously, the temperature (25 ± 0.5 °C) was monitored with a Digital Thermometer K204 Datalogger (VOLTCRAFT, Germany).

Table VI – The electrical conductivity of prepared PVB solutions.

Concentration of solution	EtOH	MetOH	THF:DMSO (9:1)	THF:DMSO (8:2)
	κ [μS/cm]	κ [μS/cm]	κ [μS/cm]	κ [μS/cm]
6 wt.%	9.2	29.9	2.4	7.8
8 wt.%	11.1	32.6	2.8	8.4
10 wt.%	12.5	37.3	3.1	9.0

5.2.2 Surface tension measurement

The surface tension of all solutions was measured via Processor Tensiometer K12 (KRÜSS GmbH, Germany). Before use, Petri dishes were washed in series of baths (20 min in each) as follows; sulphuric acid solution, distilled water, hydrochloric acid, distilled water, hydrogen peroxide solution, distilled water, acetone, distilled water and EtOH, respectively. Afterwards, the dishes were sterilized in oven at 120 °C for 20 min. To test the purity, the

measurement was carried out with EtOH, which surface tension value is tabulated (22.39 mN/m at 20 °C).

The volume of PVB solution in Petri dish was 4 ml. The surface tension of solution (Table VII) was measured with platinum probe for 180 s at 24.0 ± 0.5 °C. The platinum plate was purified by rinsing with distilled water, ethanol and distilled water again, and subsequently it was annealed in the gas burner before each measurement. To prevent MetOH and THF evaporation from solution during the experiment, the additional beaker filled with the corresponding solvent was placed into the measuring chamber. In case of PVB solutions in EtOH, it was not necessary.

Table VII – Surface tension of PVB solutions.

Concentration of solution	EtOH	MetOH	THF:DMSO (9:1)	THF:DMSO (8:2)
	γ [mN/m]	γ [mN/m]	γ [mN/m]	γ [mN/m]
6 wt.%	22.86 ± 0.02	24.31 ± 0.09	29.94 ± 0.02	31.65 ± 0.18
8 wt.%	23.06 ± 0.05	24.68 ± 0.04	31.50 ± 0.20	32.60 ± 0.20
10 wt.%	23.19 ± 0.03	24.93 ± 0.07	32.20 ± 0.20	33.70 ± 0.30

5.2.3 Rheological measurement

The rheological measurements were carried out with a Physica MCR 501 rotational rheometer (Anton Paar, Austria), equipped with C-PDT200/E a bob and cup arrangement with the inner and outer diameter 16.6 mm and 18.0 mm, respectively. The applied shear rates ranged from 0.01 to 300 $s^{-1.}$ The temperature was kept constant at 25.0 ± 0.1 °C during all experiments.

The shear viscosity corresponding to the shear rate (1.02 s^{-1}) was taken for determination of relative viscosity (eq. 9):

$$\eta_{rel} = \frac{\eta_1}{\eta_0} \tag{9}$$

where: η_{rel} is the relative viscosity [-], η_1 is the viscosity of PVB solution [Pa·s], η_0 is the viscosity of solvent [Pa·s].

The viscosity values of solvents were taken from technical data sheet [84]. For the solvents mixtures, the viscosity values were calculated from kinematic viscosity (eq. 10), which was measured with an Ubbelohde type viscometer (SI Analytics GmbH, Mainz), and density which was determined via pycnometer.

$$\nu = \frac{\eta}{\rho} \tag{10}$$

where: ν is the kinematic viscosity [mm^2/s], η is the dynamic viscosity [Pa·s], and ρ is the density [kg/cm^3].

The both measurements were performed under 23.2 ± 0.5 °C. Measured values were compared with theoretically calculated ones (Table VIII).

Table VIII – Theoretically calculated and measured values of dynamic viscosity for solvent mixtures.

Solution mixture	**Density [g/cm^3]**	**Theoretically calculated viscosity [mPa·s]**	**Measured viscosity [mPa·s]**
THF:DMSO (9:1)	0.915	0.564	0.587 ± 0.002
THF:DMSO (8:2)	0.936	0.602	0.666 ± 0.001

5.3 Electrospinning

The prepared PVB solutions were electrospun using a laboratory, self-constructed device in the Institute of Hydrodynamics AS CR (Figure 29). This device is consisted of a carbon steel rod (10 mm in diameter), and a motionless flat metal collector. The distance between tip and collector was fixed to 100 mm. A volume of the solution droplet placed onto the rod was 0.2 ml. The voltage (20 kV) was generated by a high-voltage power supply (Spellman SL70PN150, USA).

During all experiments, the temperature was 24.1 ± 0.5 °C. The relative humidity (RH) was normally kept at 41 % and subsequently increased to 65 % with the aim to prepare fibres with different morphology (chosen solutions only).

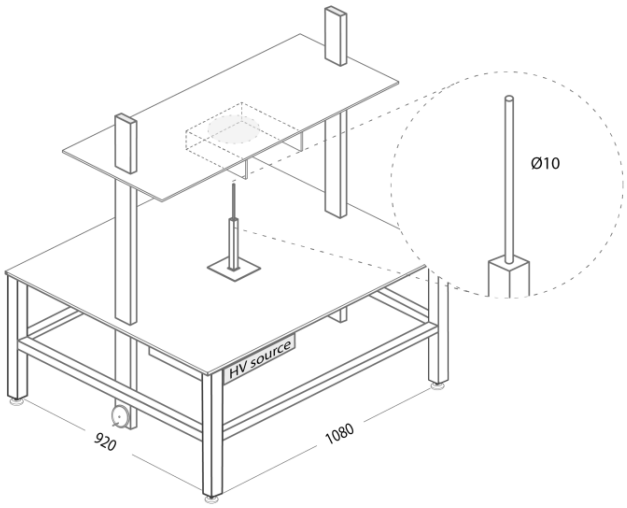

Figure 29 – A laboratory, self-constructed rod-like electrospinning device.

The electrospinning process started immediately when the voltage was applied to the electrode. The differences among particular solutions were found in the number of Taylor cones which were created on the droplet surface. When PVB was dissolved in MetOH and EtOH, the number of Taylor cones reached mostly 6 or 7. The intensive nanofibrous layer formed from fine fibres was collected on the collector. On the contrary, the fibres from PVB dissolved in THF:DMSO (9:1, and 8:2) were ejected from 4 to 6 Taylor cones only. Moreover, the intensity each of them varies, where 2 or 3 were stronger than the left ones. Thanks to this, the electrospun fibres were inhomogenously distributed in the space when the concentration of PVB was high, the fibres dried before reached the collector – so called "curtains" were formed (Figure 30). This was naturally reflected in distribution of nanofibrous layer on the collector, where the half-moon spots instead of homogenous, circular areas (MetOH, EtOH) were covered. The more homogenous nanofibrous layer would be prepared on the device where the roughness (thickness) of the layer is given by controlling of the speed on the rewind roller.

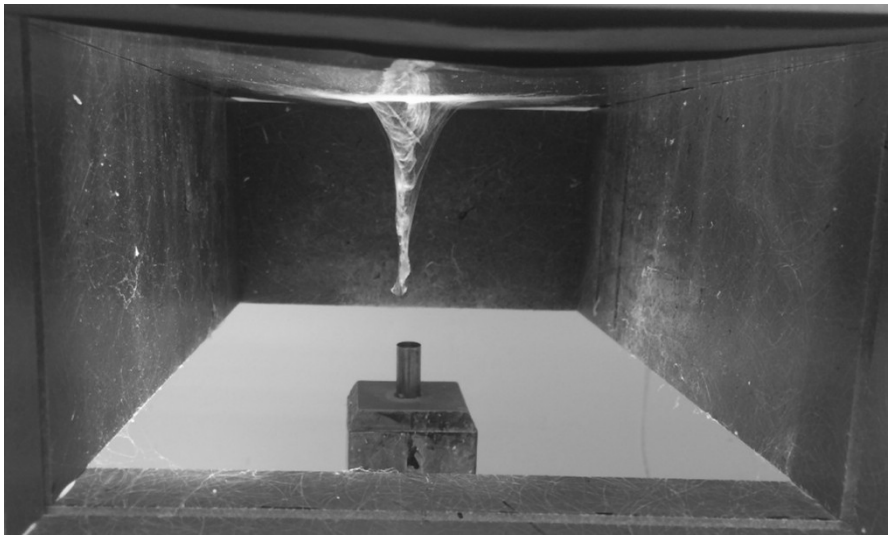

Figure 30 – Electrospun fibres collected in the space between electrode and collector, PVB dissolved in THF:DMSO (8:2) 10 wt.%.

5.4 Characterization of electrospun fibres

5.4.1 SEM analysis

The quality of electrospun fibres was evaluated using the SEM microscope VEGA 3 (Tescan, Czech Republic). Before analyzing, the fibres were coated with a conducting layer of gold to increase their conductivity. A mean diameter of prepared fibres was calculated from 300 values (3 SEM images × 100 measurements) via Adobe Creative Suite software.

5.4.2 Contact angle measurement

The wetting properties of PVB nanofibrous layers were analyzed via Drop Shape Analyzer - DSA30 (KRÜSS GmbH, Germany) equipped with a CCD camera. The volume of the water droplets was 2 μl, the temperature was 23.3 ± 0.5 °C. The contact angle was immediately obtained (Table IX) when the droplet was touched with the nanofibrous layer. In total, thirty droplets (10 droplets in 3 lines) were measured for each sample. The distance between droplets was 7 mm in line and 6 mm between the lines.

Table IX – The values of contact angle of nanofibrous layers.

Concentration of solution	EtOH	MetOH	THF:DMSO (9:1)	THF:DMSO (8:2)
	θ [°]	θ [°]	θ [°]	θ [°]
6 wt.%	138.9 ± 2.4	137.1 ± 5.2	129.2 ± 3.9	124 ± 10.4
8 wt.%	137.1 ± 3.6	134.4 ± 7.6	129.1 ± 5.3	139.0 ± 5.6
10 wt.%	137.8 ± 3.3	138.2 ± 5.8	129.4 ± 3.3	135.1 ± 6.8

To compare the influence of the morphology on the wetting behaviour, PVB films were also prepared by casting of 5 ml (8 wt.%) solution on Petri dish. The measurement was carried out by 15 droplets (5 droplets in 3 lines), where the drops distance was the same as for nanofibrous layers (Table X).

Table X – The values of contact angle of films.

Concentration of solution	EtOH	MetOH	THF:DMSO (9:1)	THF:DMSO (8:2)
	θ [°]	θ [°]	θ [°]	θ [°]
8 wt.%	76.0 ± 3.8	79.3 ± 2.6	71.5 ± 4.3	77.5 ± 3.5

6 RESULTS AND DISCUSSION

6.1 Electrical conductivity

To the important parameters, which significantly influence the quality of electrospun fibres, belongs the electrical conductivity of polymer solution. As discussed in Subchapter 1.3.5, the diameter of fibres decreases with the higher electrical conductivity.

In the Figure 31, the dependence of electrical conductivity on solution concentration is presented.

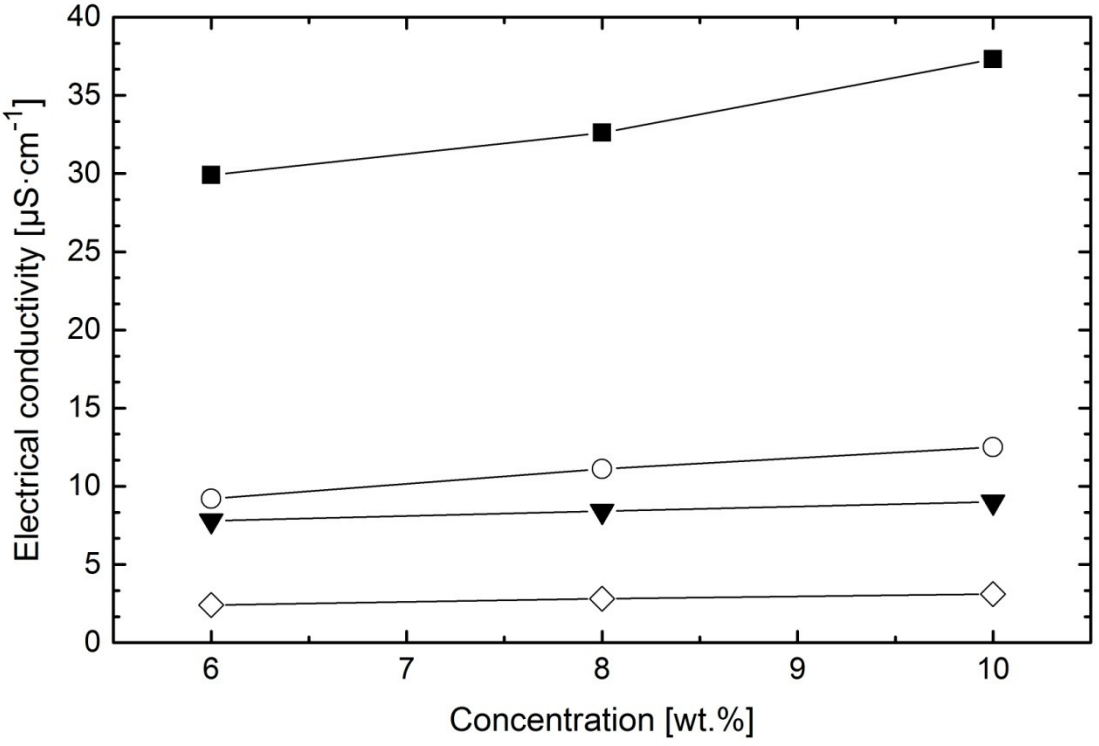

Figure 31 – Electrical conductivity *vs.* concentration of PVB dissolved in: (○) EtOH, (■) MetOH, (◇) THF:DMSO (9:1), and (▼) THF:DMSO (8:2).

Evidently, the electrical conductivity increased with the higher concentration of PVB in solutions. Probably, the trend resulted from the impurities, which PVB contained.

Moreover, a kind of selected solvent effects the electrical conductivity of PVB solutions significantly. Apparently, solubility of PVB in particular solvents connected with the degree of entanglements plays more important role than the electrical conductivity of solvent

itself. Thus, the lowest values of electrical conductivity presented for THF:DMSO (9:1) as the best solvent for PVB and contrary the highest electrical conductivity of MetOH solutions well corresponds to the solubility sequence regarding to HSP.

6.2 Surface tension

The surface tension affects the quality of electrospun fibres from defects occurrence view point. The surface tension was measured in time and correlated to an amount and a kind of solvent used in PVB solution (Table VII and Figure 32).

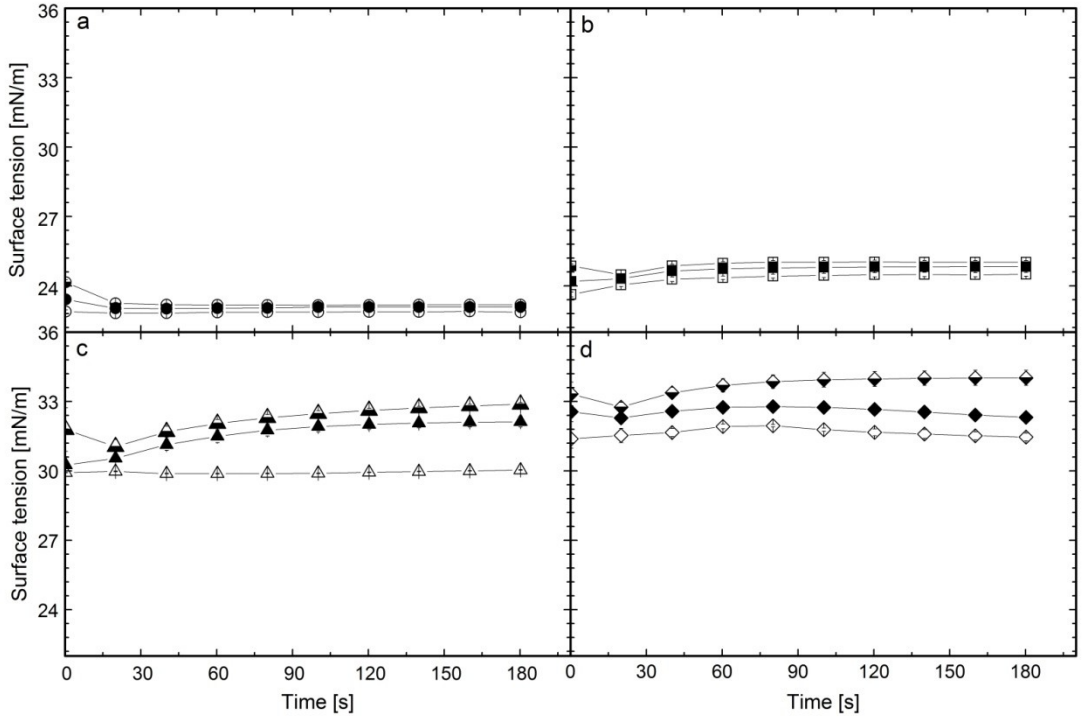

Figure 32 – The surface tension of PVB dissolved in: a) EtOH, b) MetOH, c) THF:DMSO (9:1), and d) THF:DMSO (8:2), at various concentrations: 6 wt.% (open), 8 wt.% (solid), and 10 wt.% (semi-solid) symbols.

Evidently, the surface tension slightly decreases at the beginning of the measurement and subsequently reaches the steady state. This phenomenon is more apparent at higher concentration of the PVB in solution. For further evaluation, the mean values from the whole range were calculated.

The surface tension increases with the higher concentration and simultaneously with the surface tension of the employed solvent, see in Table V. It seems that the surface tension is controlled by the solvent properties and the effect of entanglements and disentanglements, it means the solubility of PVB in the used solvents, is suppressed.

6.3 Rheological behaviour

The rheological behaviour belongs to the most frequently studied parameters of solutions employed for electrospinning, because it is strongly influenced by M_w, concentration and type of used solvent, *etc*. And thus, it has close connection to the final structure of the fibres. Here, the viscosity *vs.* the shear rate is plotted (Figure 33).

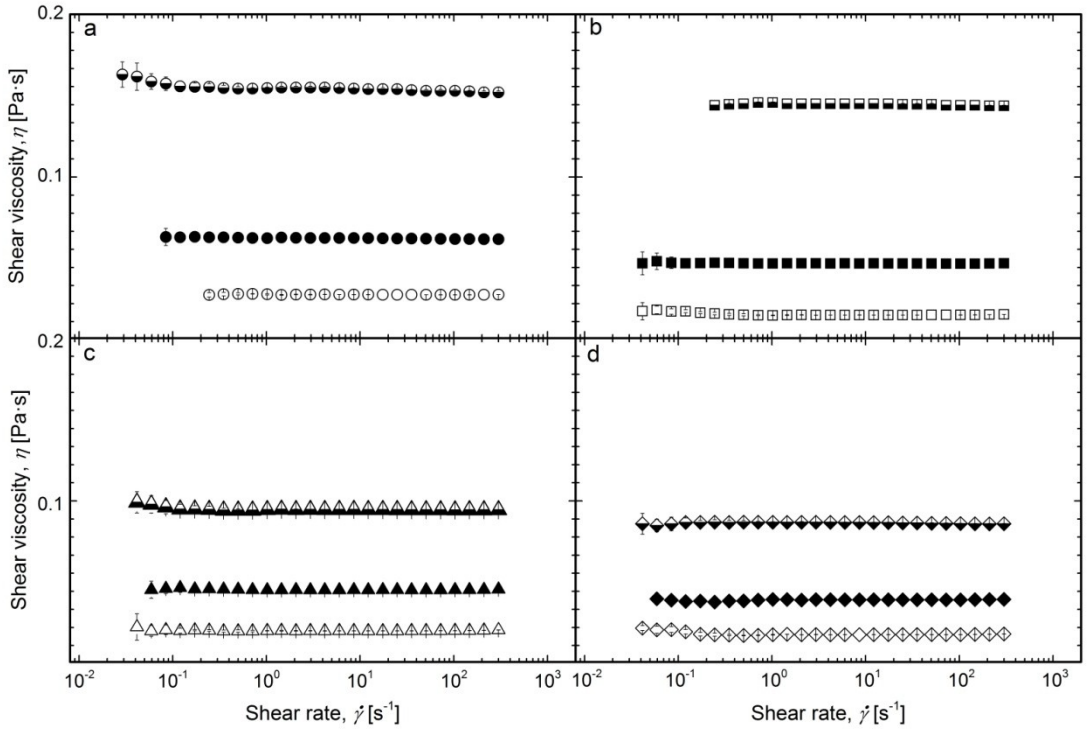

Figure 33 – The viscosity dependence on the shear rate in semi-logarithmic scale. Symbols denoted as in Figure 32.

All solutions show Newtonian behaviour nearly in the whole range of the shear rates. Deviations at low shear rate are artefact of measurement connected with the limit of the device.

The viscosity dramatically increases with the higher concentration of the PVB in the solvent. Without any doubt, the viscosity is strongly influenced by the viscosity of the solvent. On the other hand, the strong contribution of solubility of PVB in the solvent is also expected. To clarify this contribution, the relative viscosity was calculated and presented in Figure 34.

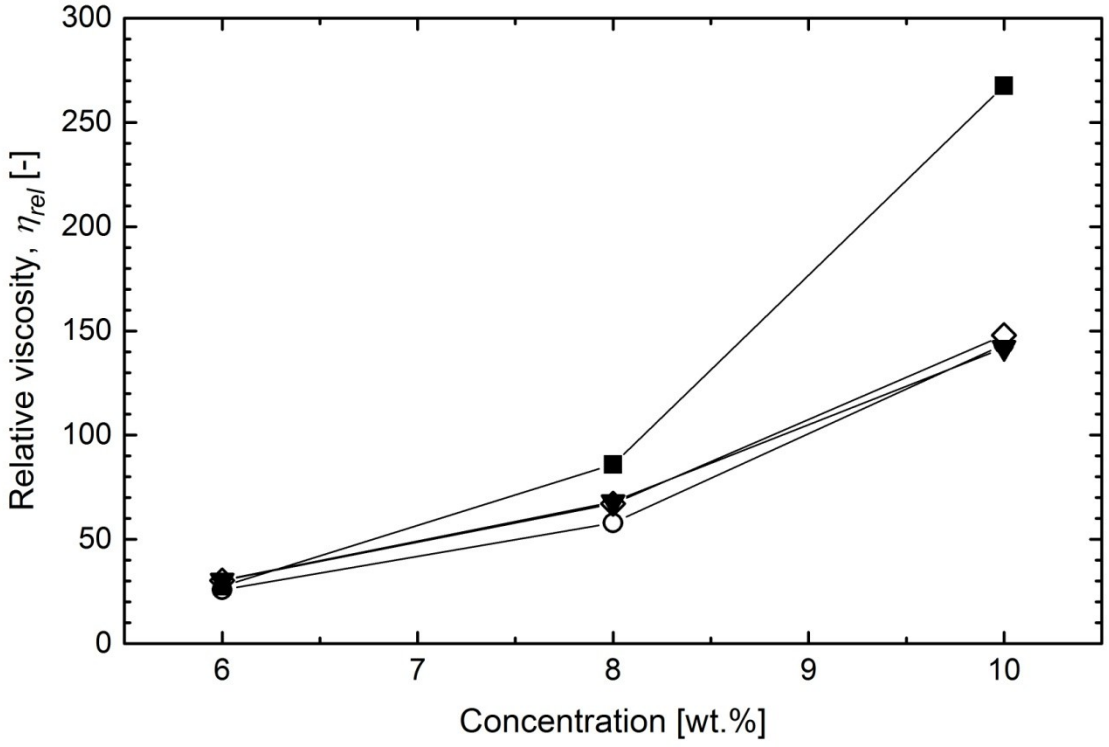

Figure 34 – The dependence of relative viscosity on concentration of PVB in solutions. Symbols as denoted in Figure 31.

When the concentration of PVB in solution approaches to zero, the real behaviour of the polymer in the solvent can be estimated. In the case of the good solvents (THF:DMSO), the polymer chains are disentanglement and the viscosity increases. On the other hand, when the PVB is dissolved in the poor solvents (MetOH, EtOH), the polymer chains stay

in contracted conformation. Therefore, the viscosity is lower than in the case of the good solvents.

In consideration to higher concentration of PVB in solution, there is no clear answer, whether the viscosity of PVB solvents at concentration range from 6 to 10 wt.% is controlled by solvents viscosity or the solubility of PVB in particular solvents.

6.4 Morphology of polyvinylbutyral fibres

Finally, PVB solutions differing in a kind of employed solvent and its concentration were electrospun and prepared fibres were characterized via SEM.

Irrespectively to the kind of the solvent, the diameter of the fibres was found to increase with higher concentration of PVB in solutions (Figures 35 – 41). It is a result of higher solution viscosity (confirmed by previous measurements), which hinders the thinning of the fibres during the electrospinning.

Besides the morphology of electrospun fibres, the higher content of PVB has a positive impact on their quality. The amount of the beads defects is significantly reduced. The particular fibres seem to be more homogenous in longitudinal direction. Simultaneously, the mean distribution rises (Figures 35c – 40c, 41).

Apart from the concentration, a kind of solvent used for the PVB solution dramatically influences the morphology of the electrospun fibres. When the PVB was dissolved in rather poor solvents (MetOH and EtOH), very fine PVB fibres are produced (Figures 35, 36). On the hand, the good solvent ensures thicker and less defective fibres, which can be explained by higher disentanglements of PVB chains within it. This contributes to their better spinnability.

Another difference is the shape of the beads defects if appear. Rather elongated beads defects occur on fibres from PVB in EtOH, which contrast to more frequent and circular beads on fibres from PVB in MetOH. The presence of large beads appears on the fibres from PVB in THF:DMSO solutions at lower concentration. In more detail (Figure 35c), the morphology of fibres from PVB solution in EtOH is flat and subsequently rolled into circular form.

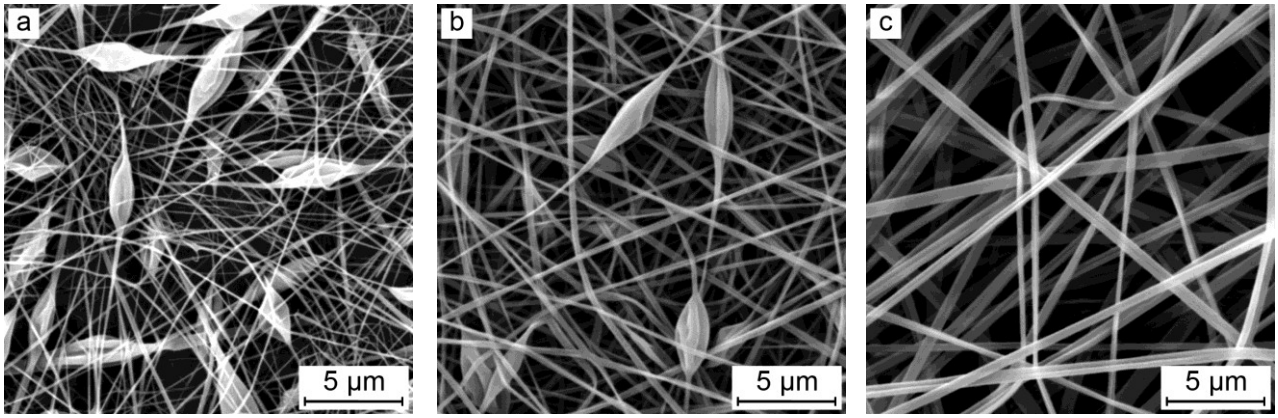

Figure 35 – The electrospun fibres from PVB dissolved in EtOH (RH = 41 %): a) 6 wt.%, b) 8 wt.%, and c) 10 wt.%.

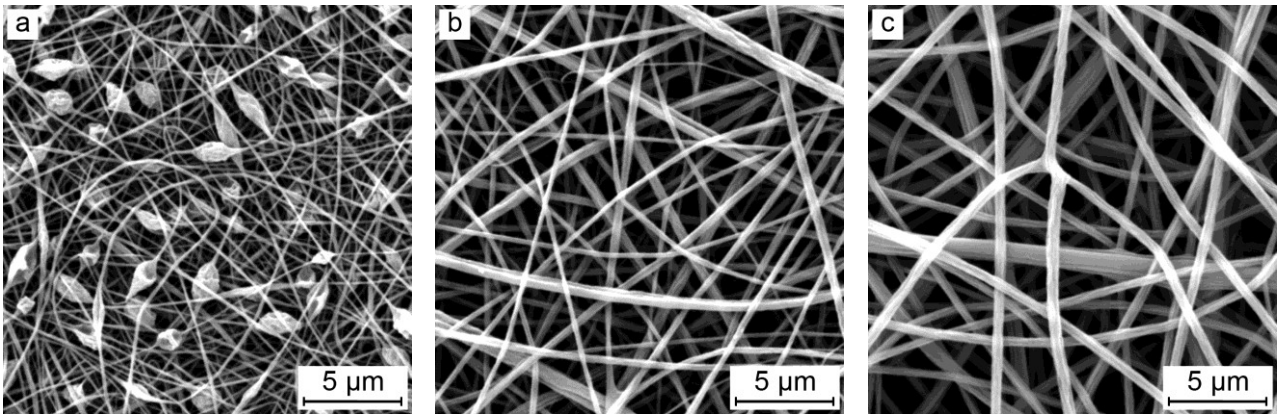

Figure 36 – The electrospun fibres from PVB dissolved in MetOH (RH = 41 %): a) 6 wt.%, b) 8 wt.%, and c) 10 wt.%.

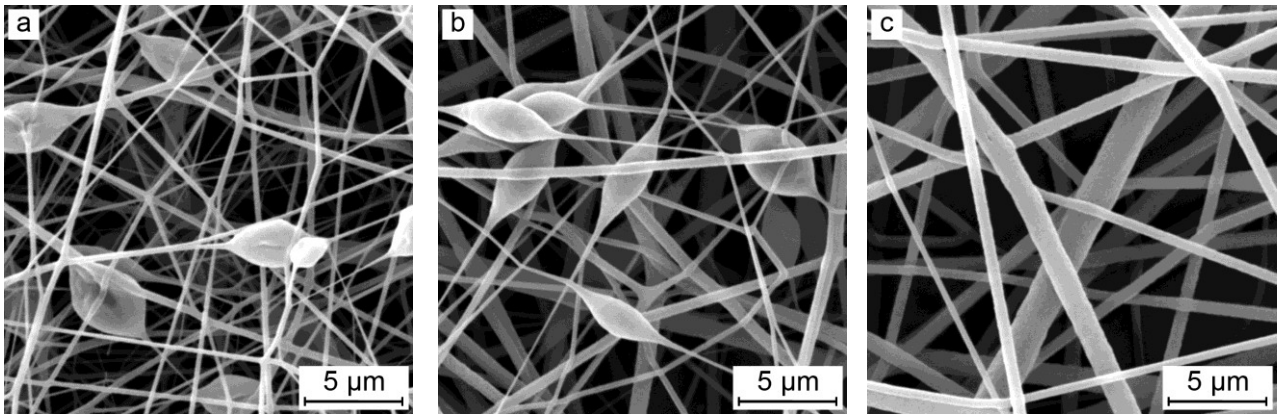

Figure 37 – The electrospun fibres from PVB dissolved in THF:DMSO (9:1) (RH = 41 %): a) 6 wt.%, b) 8 wt.%, and c) 10 wt.%.

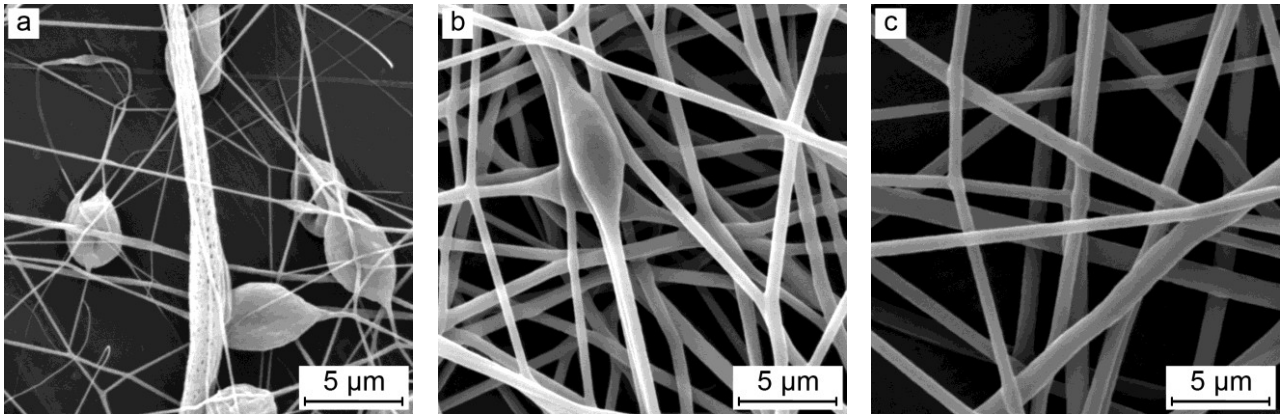

Figure 38 – The electrospun fibres from PVB dissolved in THF:DMSO (9:1) (RH = 65 %): a) 6 wt.%, b) 8 wt.%, and c) 10 wt.%.

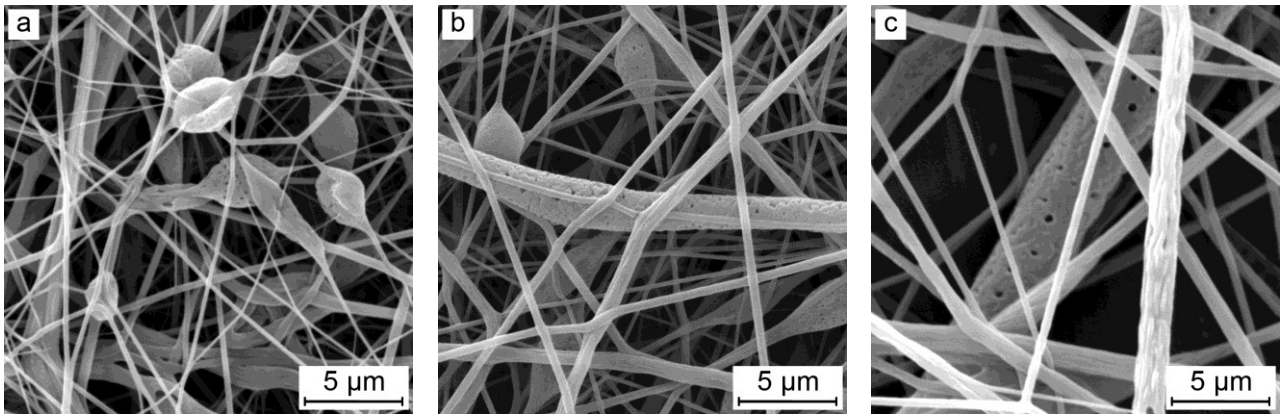

Figure 39 – The electrospun fibres from PVB dissolved in THF:DMSO (8:2) (RH = 41 %): a) 6 wt.%, b) 8 wt.%, and c) 10 wt.%.

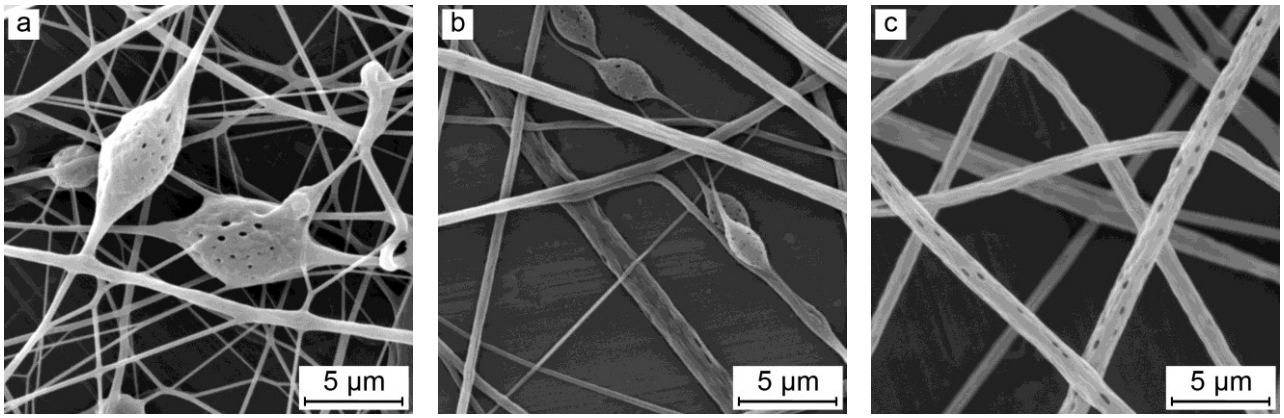

Figure 40 – The electrospun fibres from PVB dissolved in THF:DMSO (8:2) (RH = 65 %): a) 6 wt.%, b) 8 wt.%, and c) 10 wt.%.

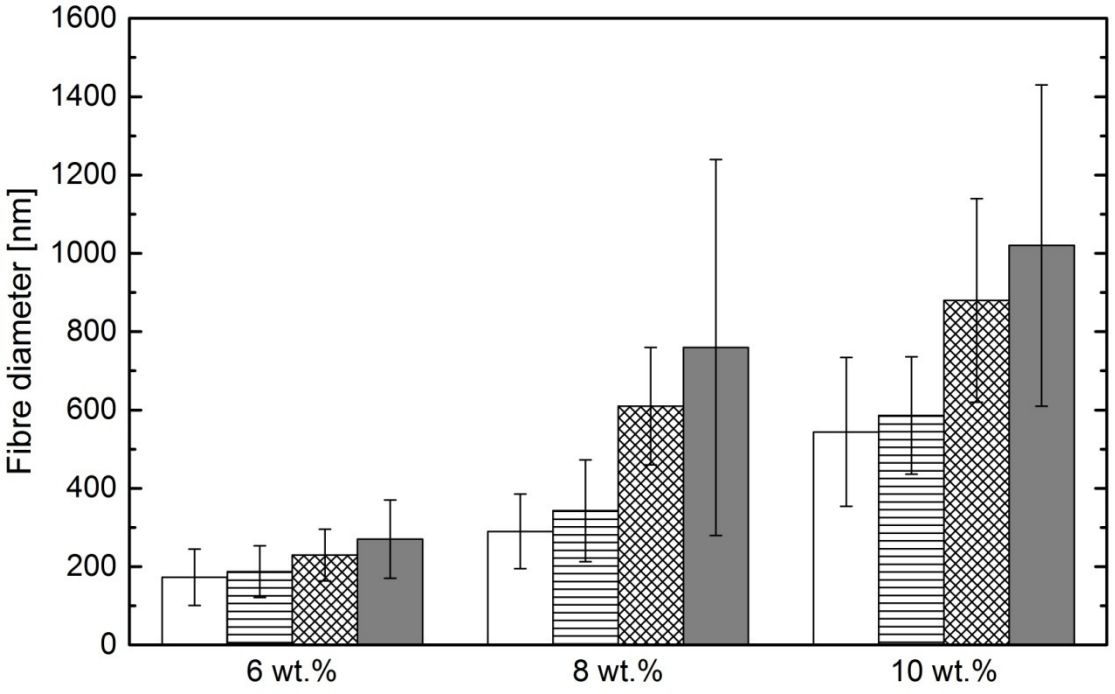

Figure 41 – The dependence of fibres diameter on concentration of PVB dissolved in: EtOH (white), MetOH (linear hatching), THF:DMSO (9:1) (cross hatching), and THF:DMSO (8:2) (grey).

6.5 The effect of humidity

To prepare the fibres with porous structures, PVB was dissolved in a mixture of a good solvents containing small amount of a poor solvent, namely THF:DMSO in volume ratios 9:1 and 8:2 and spun under various humidity – 41 % and 65 %. Both solvents differ also in boiling point (66 °C and 189 °C, respectively).

Evidently, the PVB solution prepared from the solvent mixture THF:DMSO 9:1 presented the porous structure only when they were spun under the higher humidity (65 %) (Figures 37 and 38). On the contrary, when the concentration of a poor solvent was higher (THF:DMSO 8:2), the porous structure was observed even at lower humidity (Figures 39 and 40). Apparently, the higher concentration of PVB in solutions positively contributes to higher amount of pores along the fibres structure.

6.6 The mapping of nanofibrous layers

The surface of nanofibrous layers is inhomogeneous due to the irregularities in the collection of nanofibrous layer on the collector during the electrospinning (explained in Subchapter 5.3). Thus, the nanofibrous layers with variable roughness are obtained, which is reflected in wetting properties at various positions. Therefore, the mapping diagrams covering larger area were created for more accurate determination of contact angles on nanofibrous layers (Figures 42–44).

The rougher layer corresponds to the higher value of contact angles. Moreover, the droplet could be held by fluff of fibres sticking out from the nanofibrous layer, which presents nearly superhydrophobic behaviour as shown the fibres from PVB/(THF:DMSO, 8:2) in Figure 44c.

However, the observed results (SEM analysis as well as contact angle measurements) showed the strong dependence on the roughness of measured nanofibrous layer. Thus, the impact of porous structure on improvement of nanofibrous layers hydrophobicity was not confirmed as presented in literature review. The possible reason could be connected to the process parameters (low atmospheric pressure, which was out of control, *etc.*) during the electrospinning.

In contrast to rather hydrophobic nanofibrous layers, the films showed the hydrophilic behaviour despite the fact that the same solutions were employed for their preparation (Figure 45). The possible explanation could be given by roughness variance surface – very rough fibres contrasting with smooth films.

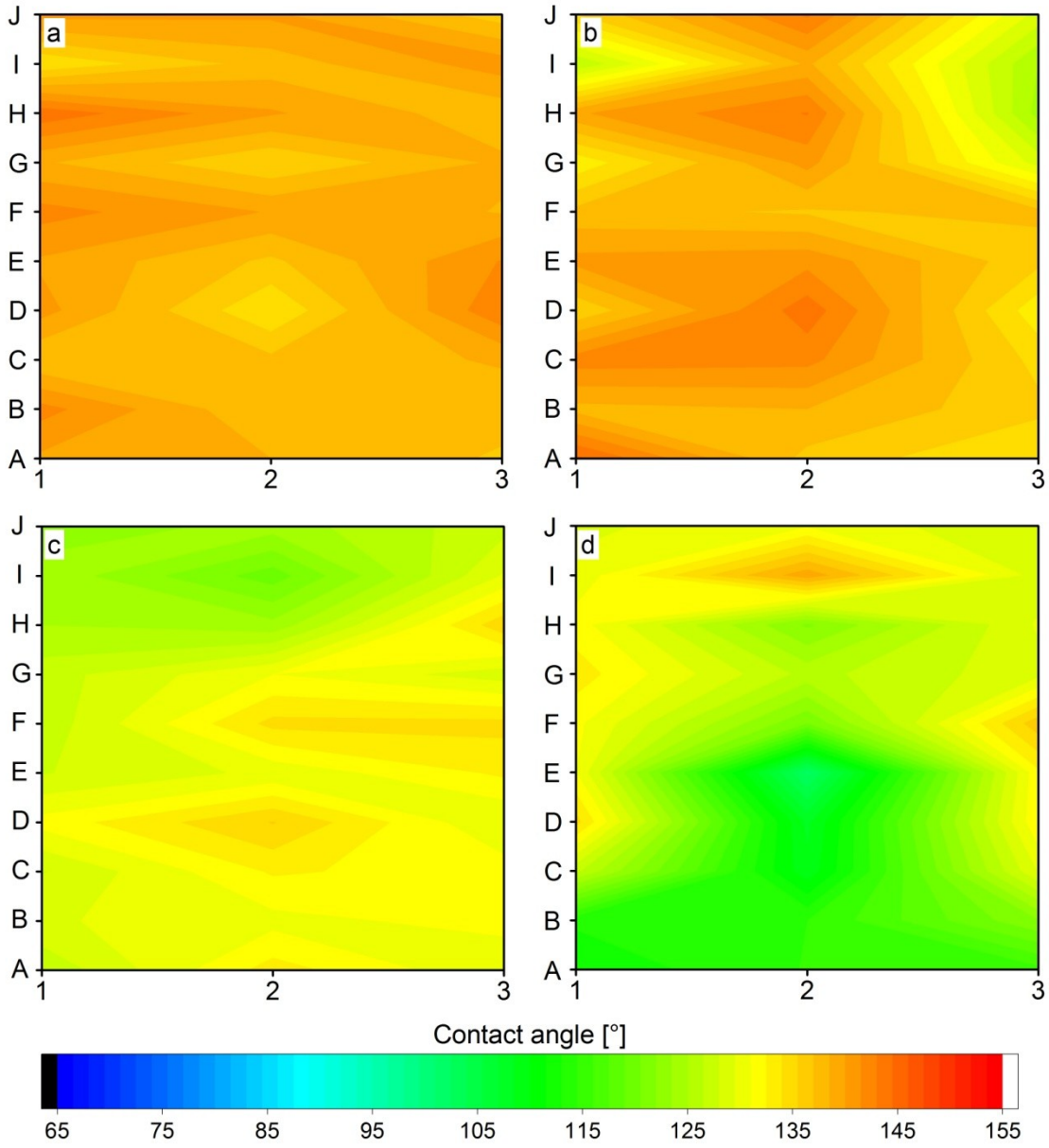

Figure 42 – Mapped surface of nanofibrous layers prepared from 6 wt.%: a) PVB/EtOH (RH = 41 %), b) PVB/MetOH (RH = 41 %), c) PVB/(THF:DMSO, 9:1) (RH = 65 %), and d) PVB/(THF:DMSO, 8:2) (RH = 65 %) solution.

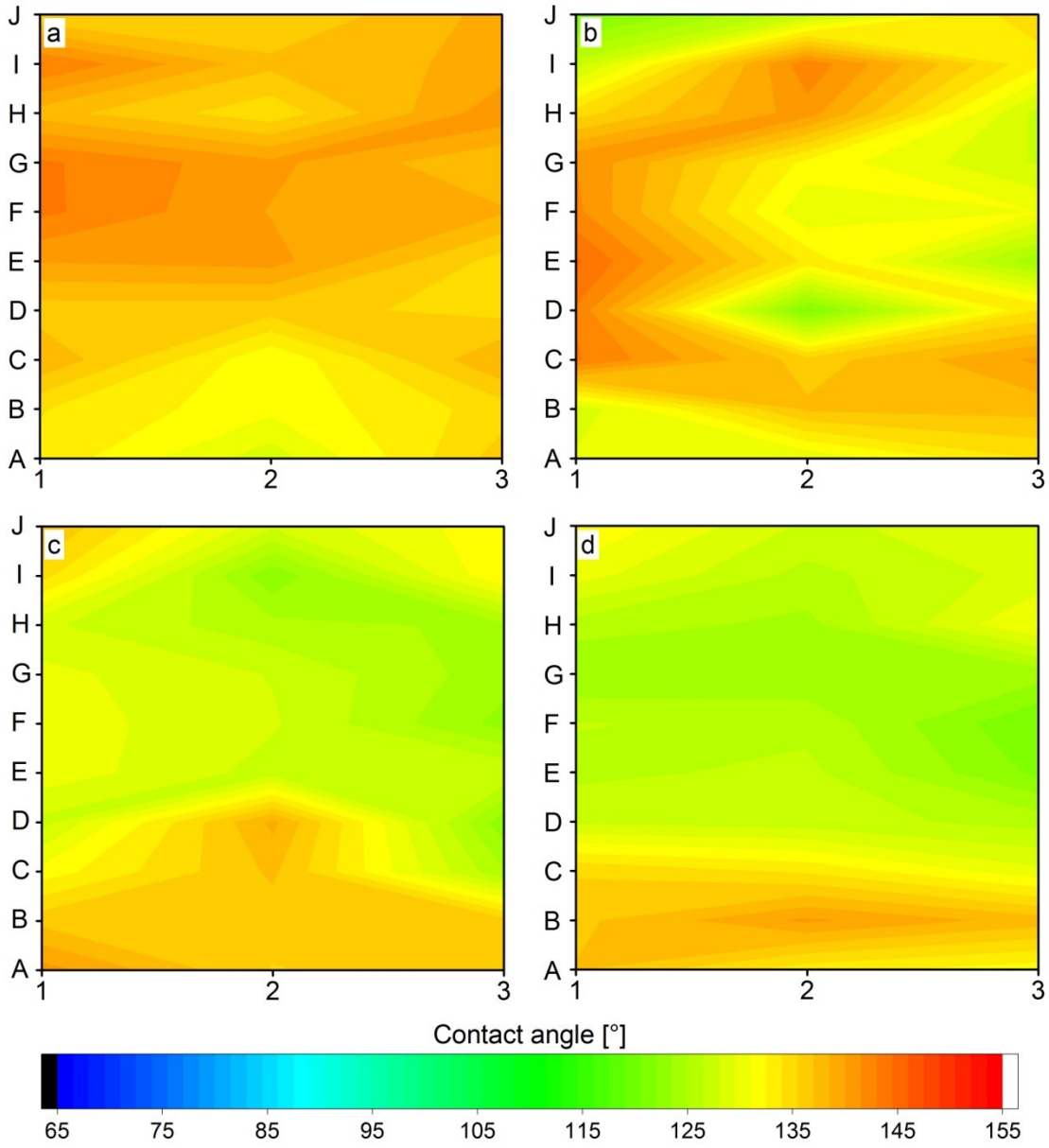

Figure 43 – Mapped surface of nanofibrous layers prepared from 8 wt.%: a) PVB/EtOH (RH = 41 %), b) PVB/MetOH (RH = 41 %), c) PVB/(THF:DMSO, 9:1) (RH = 65 %), and d) PVB/(THF:DMSO, 8:2) (RH = 65 %) solution.

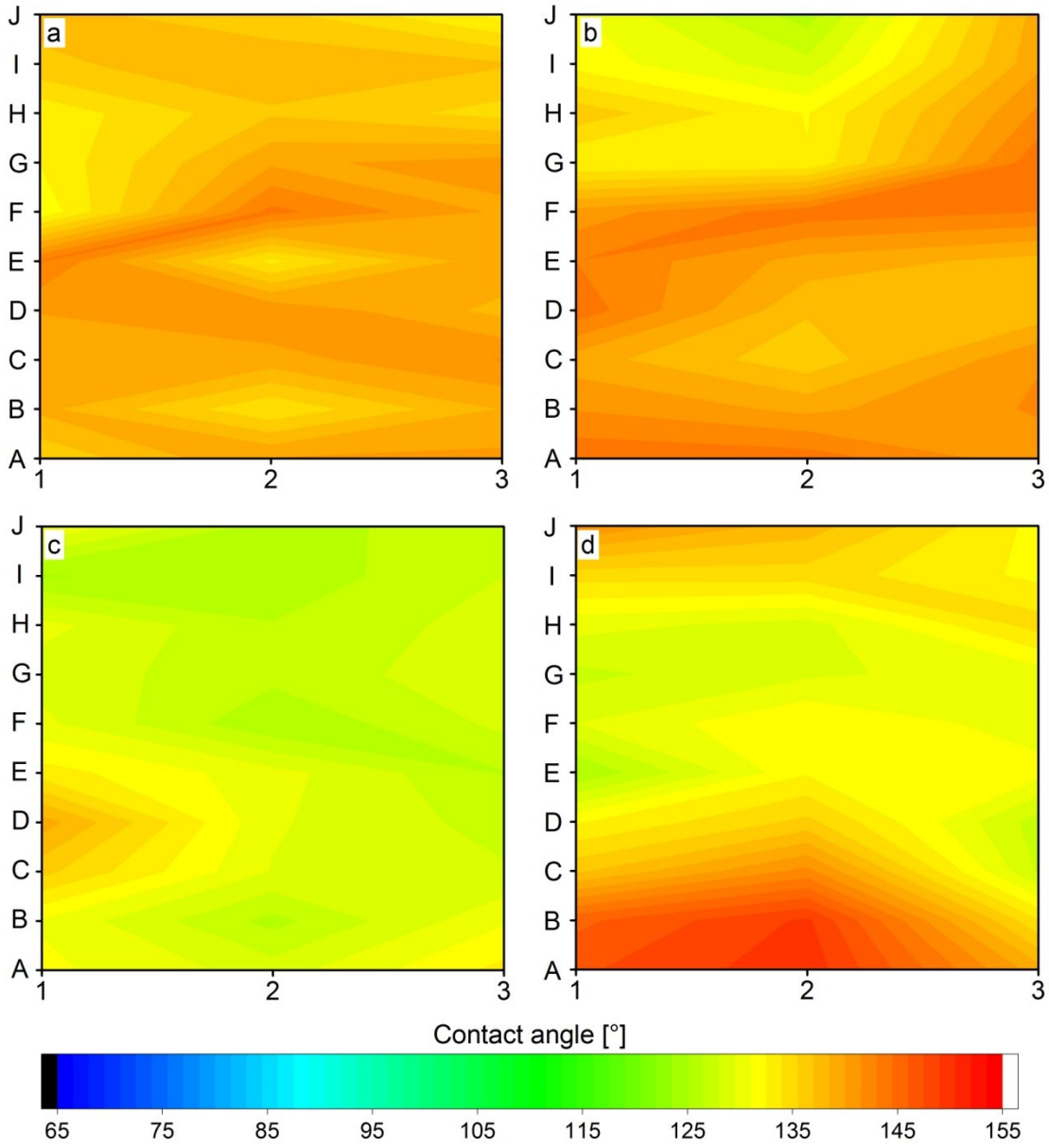

Figure 44 – Mapped surface of nanofibrous layers prepared from 10 wt.%: a) PVB/EtOH (RH = 41 %), b) PVB/MetOH (RH = 41 %), c) PVB/(THF:DMSO, 9:1) (RH = 65 %), and d) PVB/(THF:DMSO, 8:2) (RH = 65 %) solution.

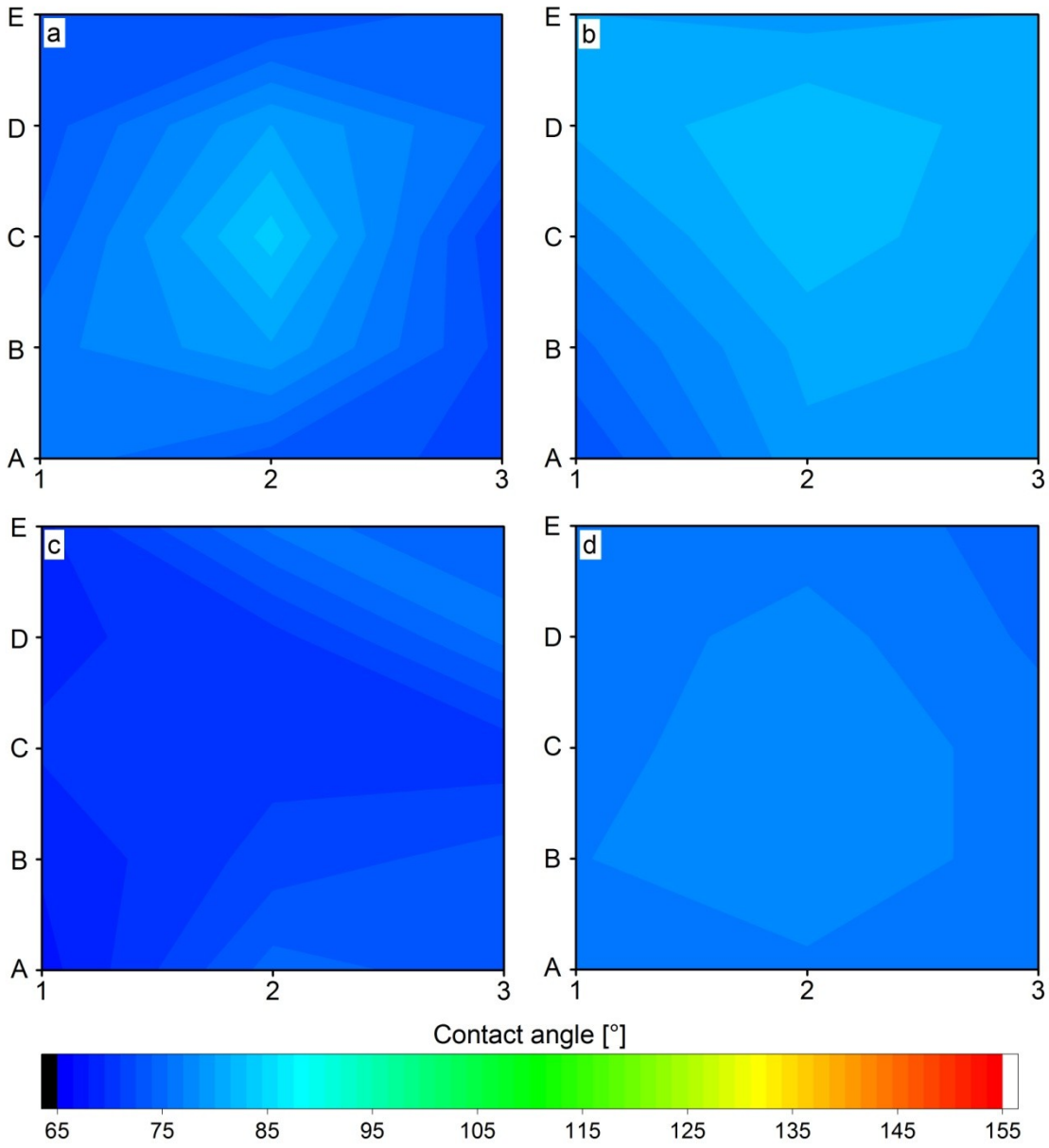

Figure 45 – Mapped surface of films prepared from 8 wt.%: a) PVB/EtOH, b) PVB/MetOH, c) PVB/(THF:DMSO, 9:1), and d) PVB/(THF:DMSO, 8:2) solution.

6.7 Evaluation of solution parameters and wettability on fibres diameter

In this Subchapter, the effect of measured parameters on fibres diameter and subsequently on wettability presented by contact angles was compared (Figure 46–48).

PVB dissolved in good solvents (mixture of THF:DMSO in volume ratios 9:1, 8:2) show lower electrical conductivity but higher surface tension, which decelerate the electrospinning process. As a result, fibres with higher diameter are electrospun. This fact is confirmed to lower viscosity, too. In the case of the poor solvents (EtOH, MetOH), the behaviour is exactly opposite. All parameters, namely electrical conductivity, surface tension and dynamic viscosity, are increased with higher concentration of the PVB in solutions regardless to particular solvents.

The nanofibrous layers prepared from PVB dissolved in poor solvent present negligibly higher hydrophobicity.

The dynamic viscosity was plotted in [mPa·s], and fibres diameter was divided by 10 for better representation.

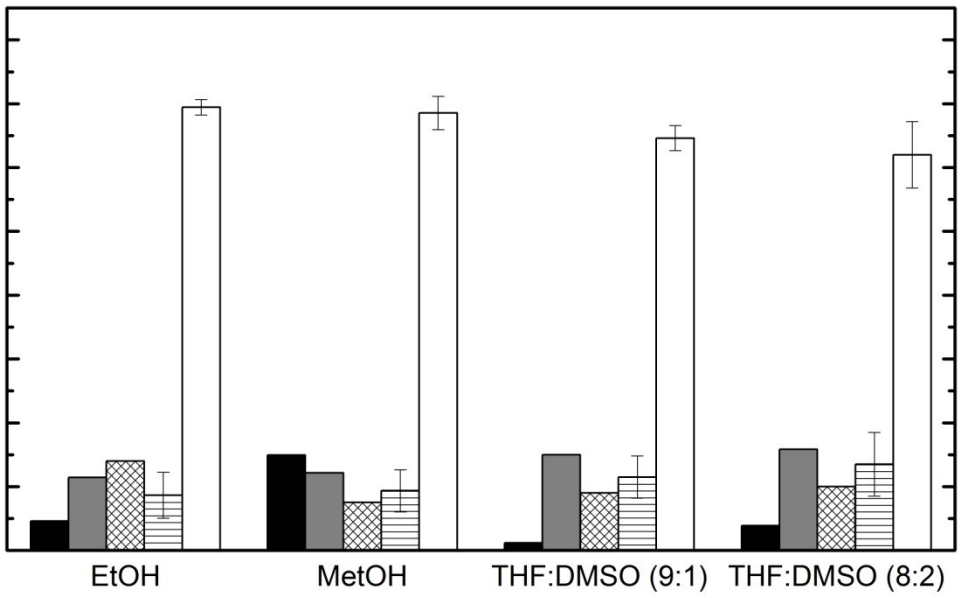

Figure 46 – The summary of PVB solution (6 wt.%) and fibres characterizations: electrical conductivity (black), surface tension (grey), viscosity (cross hatching), fibre diameter (linear hatching), and contact angle (white).

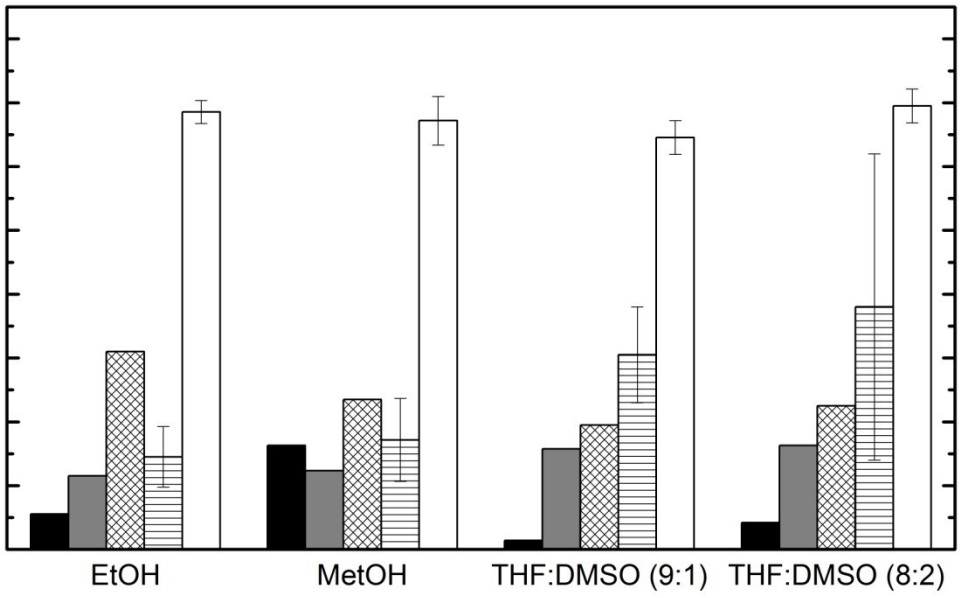

Figure 47 – The summary of PVB solution (8 wt.%) and fibres characterizations: electrical conductivity (black), surface tension (grey), viscosity (cross hatching), fibre diameter (linear hatching), and contact angle (white).

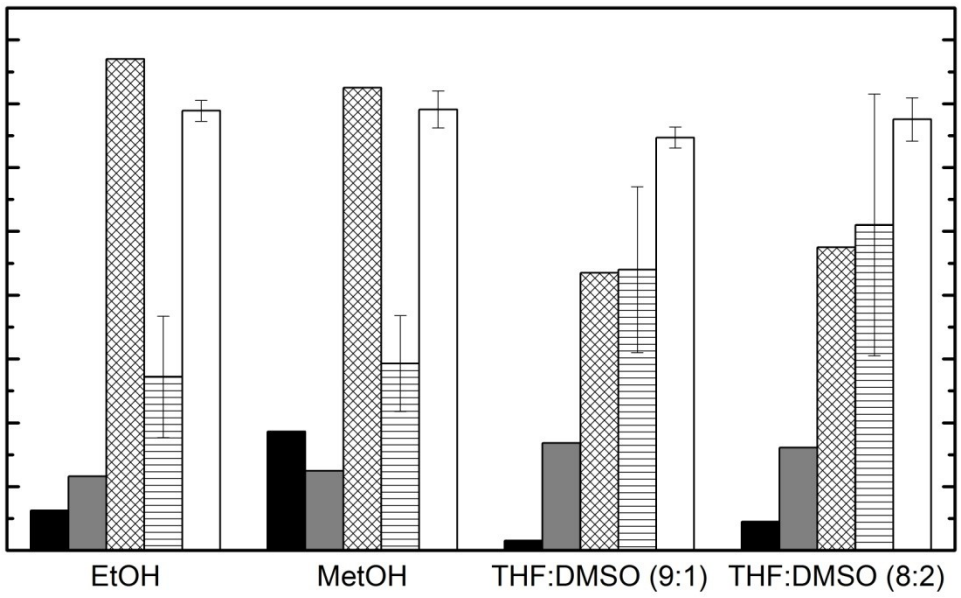

Figure 48 – The summary of PVB solution (10 wt.%) and fibres characterizations: electrical conductivity (black), surface tension (grey), viscosity (cross hatching), fibre diameter (linear hatching), and contact angle (white).

CONCLUSION

Presented study was focused on preparation of nanofibres and nanofibrous layers from PVB solutions via electrospinning to demonstrate the positive impact of improved, porous structure on hydrophobicity. The solutions were prepared by dissolution of PVB in two solvents and two mixtures of it, namely in EtOH, MetOH (poor solvents), and mixtures of THF:DMSO in ratios 9:1, and 8:2 (good solvents), respectively.

The lower electric conductivity connected with higher surface tension presented by PVB dissolved in good solvents is reflected in higher mean diameter of the fibres (600 ± 200 nm). Opposite behaviour connected with markedly thinner fibres (350 ± 120 nm) showed PVB dissolved in poor solvents.

Thy hydrophobicity represented by contact angle of PVB solutions was measured. No significant difference between hydrophobicity of PVB dissolved in poor solvents (138 ± 5°) and PVB dissolved in good solvents (131 ± 6°), respectively was monitored. Evidently, the fibres with improved porosity providing the higher hydrophobicity, or even superhydrophobicity, were not electrospun.

BIBLIOGRAPHY

[1] RAMAKRISHNA, S., FUJIHARA, K., TEO, W. E., LIM, T. C., MA, Z. *An introduction to electrospinning and nanofibers*. Singapore: World Scientific, 2005.

[2] HUANG, Z. M., ZHANG, Y.-Z., KOTAKI, M., RAMAKRISHNA, S. A review on polymer nanofibers by electrospinning and their applications in nanocomposites. *Composites Science and Technology*. 2003, Vol. 63, p. 2223–2253.

[3] RENEKER, D. H., CHUN, I. Nanometre diameter fibres of polymer, produced by electrospinning. *Nanotechnology*, 1996. Vol. 7.3, p. 216.

[4] LI, Z., WANG, C. *One-dimensional nanostructures: Electrospinning technique and unique nanofibers*.New York: Springer, 2013. ISBN 978-3-642-36426-6.

[5] YENER, F., JIRSAK, O. Fabrication and optimization of polyvinyl butyral nanofibres produced by roller electrospinning. In: *12th AUTEX World Textile Conference, Book of Proceedings,* Croatia. 2012. p. 251−256.

[6] FORMHALS, A. *Production of artificial fibers from fiber formin liquids*. U.S. Patent No 2,323,025, 1943.

[7] BHARDWAJ, N., KUNDU, S. C. Electrospinning: A fascinating fiber fabrication technique. *Biotechnology Advances*. 2010. Vol. 28, p. 325–347.

[8] SIMONS, H. L. *Process and apparatus for producing patterned non-woven fabrics*. U.S. Patent No 3,280,229, 1966.

[9] BAUMGARTEN, P. K. Electrostatic spinning of acrylic microfibers. *Journal of colloid and interface science*, 1971. Vol. 36.1, p. 71–79.

[10] JIRSAK, O., SANETRNIK, F., LUKAS, D., KOTEK, V., MARTINOVA, L., CHALOUPEK, J. *Method of nanofibres production from a polymer solution using electrostatic spinning and a device for carrying out the method*. U.S. Patent No 7,585,437, 2009.

[11] DI, J., ZHAO, Y., YU, J. Fabrication of molecular sieve fibers by electrospinning. *Journal of Materials Chemistry*, 2011. Vol. 21.24, p. 8511–8520.

[12] ZONG, X., KIM, K., FANG, D., RAN, S., HSIAO, B. S., CHU, B. Structure and process relationship of electrospun bioabsorbable nanofiber membranes. *Polymer*, 2002. Vol. 43.16, p. 4403–4412.

[13] TAN, S. H., INAI, R., KOTAKI, M., RAMAKRISHNA, S. Systematic parameter study for ultra-fine fiber fabrication via electrospinning process. *Polymer*, 2005, Vol. 46, p. 6128–6134.

[14] DEITZEL, J. M., KLEINMEYER, J., HARRIS, D., BECK TAN, N. C. The effect of processing variables on the morphology of electrospun nanofibers and textiles. *Polymer,* 2001. Vol. 42, p. 261–272.

[15] KOSKI, A., YIM, K., SHIVKUMAR, S. Effect of molecular weight on fibrous PVA produced by electrospinning. *Materials Letters*, 2004. Vol. 58.3, p. 493–497.

[16] AFSHARI, M. Electrospun nanofibers, *Woodhead publishing series in textiles.* Vol. 185. ISBN 978-0-08-100907-9.

[17] HANSEN, C. M. *Hansen solubility parameters: A user's handbook* (2nd ed.), CRC Press, Taylor & Francis Group, USA, 2007.

[18] STENICKA, M., PEER, P., FILIP, P., PAVLINEK, V., MACHOVSKY, M. Electrospinning of PVB solved in methanol and isopropanol. *5th WSEAS International Conference on Materials Science*, Sliema, 2012.

[19] LUBASOVA, D., MARTINOVA, L. Controlled morphology of porous polyvinyl butyral nanofibers. *Journal of Nanomaterials*, 2011.

[20] FONG, H., CHUN, I., RENEKER, D. H. Beaded nanofibers formed during electrospinning. *Polymer*, 1999. Vol. 40.16, p. 4585–4592.

[21] DOSHI, J., RENEKER, D. D. Electrospinning process and applications of electrospun fibers, *Journal of Electrostatics.*1995. Vol. 35, p. 151–160.

[22] XIE, J., TAN, R. S., WANG, C. H. Biodegradable microparticles and fiber fabrics for sustained delivery of cisplatin to treat C6 glioma in vitro. *Journal of Biomedical Materials Research Part A*, 2008. Vol. 85.4, p. 897–908.

[23] YENER, F., JIRSAK, O. Comparison between the needle and roller electrospinning of polyvinylbutyral. *Journal of Nanomaterials*, 2012.

[24] CMAROVA, A. *Nanowebs and thin films based on poly(ethylene) oxide.* Zlin, 2015. Bachelor thesis.

[25] SUKIGARA, S., GANDHI, M., AYUTSEDE, J., MICKLUS, M., KO, F. Regeneration of Bombyx mori silk by electrospinning-part 1: Processing parameters and geometric properties. *Polymer*, 2003. Vol. 44, p. 5721–5727.

[26] LEE, K. H., KIM, H. Y., KHIL, M. S., RA, Y. M., LEE, D. R. Characterization of nano-structured poly (ε-caprolactone) nonwoven mats via electrospinning. *Polymer*, 2003. Vol. 44, p. 1287–1294.

[27] SILL, T. J., VON RECUM, H. A. Electrospinning: Applications in drug delivery and tissue engineering. *Biomaterials*, 2008. Vol. 29, p. 1989–2006.

[28] CASPER, C. L., STEPHENS, J. S., TASSI, N. G., CHASE, D. B., RABOLT, J. F. Controlling surface morphology of electrospun polystyrene fibers: Effect of humidity and molecular weight in the electrospinning process. *Macromolecules*, 2004, Vol. 37, p. 573–578.

[29] SASITHORN, N., MARTINOVA, L. Fabrication of silk nanofibres with needle and roller electrospinning methods. *Journal of Nanomaterials*, 2014.

[30] CENGIZ-ÇALLIOĞLU, F. Dextran nanofiber production by needleless electrospinning process. *Polymers*. 2014. Vol. 14.

[31] PEER, P., STENICKA, M., PAVLINEK, V., FILIP, P., KURITKA, I., BRUS, J. An electrorheological investigation of PVB solutions in connection with their electrospinning qualities. *Polymer Testing*. 2014. Vol. 39, p. 115–121.

[32] JIRSAK, O., PETRIK, S. Recent advances in nanofibre technology: Needleless electrospinning. *International Journal of Nanotechnology*, 2012, Vol. 9, p. 836–845.

[33] KURECIC, M., SMOLE, M. S. Electrospinning: Nanofibre production method. *Tekstilec*, 2013, p. 4–121.

[34] *Intergrating nanofibres into filtration media* [online]. [Accessed 5 February 2017]. Available from: http://www.filtsep.com/view/4480/integrating-nanofibres-into-filtration-media/

[35] RHO, K. S., JEONG, L., LEE, G., SEO, B. M., PARK, Y. J., HONG, S. D., ROH, S., CHO, J. J., PARK, W. H., MIN, B. M. Electrospinning of collagen nanofibers: Effects on the behavior of normal human keratinocytes and early-stage wound healing. *Biomaterials*. 2006. Vol. 27, p. 1452–1461.

[36] MATTHEWS, J. A., WNEK, G. E., SIMPSON, D. G., BOWLIN, G. L. Electrospinning of collagen nanofibers. *Biomacromolecules*. 2002. Vol. 3, p. 232–238.

[37] MA, Z., KOTAKI, M., RAMAKRISHNA, S. Electrospun cellulose nanofiber as affinity membrane. *Journal of Membrane Science*. 2005. Vol. 265, p. 115–123.

[38] KIM, C. W., KIM, D. S., KANG, S. Y., MARQUEZ, M., JOO, Y. L. Structural studies of electrospun cellulose nanofibers. *Polymer*. 2006. Vol. 47, p. 5097–5107.

[39] DEITZEL, J. M., KLEINMEYER, J. D., HIRVONEN, J. K., BECK TAN, N. C. Controlled deposition of electrospun poly(ethylene oxide) fibers. *Polymer*. 2001. Vol. 42, p. 8163–8170.

[40] SON, W. K., YOUK, J. H., LEE, T. S., PARK, W. H.. The effects of solution properties and polyelectrolyte on electrospinning of ultrafine poly(ethylene oxide) fibers. *Polymer*. 2004. Vol. 45, p. 2959–2966.

[41] HOU, H., GE, J. J., ZENG, J., LI, Q., RENEKER, D. H., GREINER, A., CHENG, S. Z. D. Electrospun polyacrylonitrile nanofibers containing a high concentration of well-aligned multiwall carbon nanotubes. *Chemistry of Materials*. 2005. Vol. 17, p. 967–973.

[42] STACHEWICZ, U., BARBER, A. H. Enhanced wetting behavior at electrospun polyamide nanofiber surfaces. *Langmuir*. 2011. Vol. 27, p. 3024–3029.

[43] SUPAPHOL, P., MIT-UPPATHAM, C., NITHITANAKUL, M. Ultrafine Electrospun Polyamide-6 Fibers: Effects of solvent system and emitting electrode polarity on morphology and average fiber diameter. *Macromolecular Materials and Engineering*. 2005. Vol. 290, p. 933–942.

[44] LEE, K. H., KIM, H. Y., BANG, H. J., JUNG, Y. H., LEE, S. G. The change of bead morphology formed on electrospun polystyrene fibers. *Polymer*. 2003. Vol. 44, p. 4029–4034.

[45] DEMIR, M. M., YILGOR, I., YILGOR, E., ERMAN, B. Electrospinning of polyurethane fibers. *Polymer*. 2002. Vol. 43, p. 3303–3309.

[46] PEDICINI, A., FARRIS, R. J. Mechanical behavior of electrospun polyurethane. *Polymer*. 2003. Vol. 44, p. 6857–6862.

[47] KHIL, M. S., CHA, D. I., KIM, H. Y., KIM, I. S., BHATTARAI, N. Electrospun nanofibrous polyurethane membrane as wound dressing. *Journal of Biomedical Materials Research Part B: Applied Biomaterials*. 2003. Vol. 67B, p. 675–679.

[48] BOGNITZKI, M., BECKER, M., GRAESER, M., MASSA, W., WENDORFF, J. H., SCHAPER, A., WEBER, D., BEYER, A., GÖLZHÄUSER, A., GREINER, A. Preparation of sub-micrometer copper fibers via electrospinning. *Advanced Materials*, 2006. Vol. 18, p. 2384–2386.

[49] LI, D., XIA, Y. Direct fabrication of composite and ceramic hollow nanofibers by electrospinning. *Nano letters*, 2004. Vol. 4.5, p. 933–938.

[50] INAGAKI, M., YANG, Y., KANG, F. Carbon nanofibers prepared via electrospinning. *Advanced Materials*, 2012. Vol. 24.19, p. 2547–2566.

[51] KIM, I. D., ROTHSCHILD, A., LEE, B. H., KIM, D. Y., JO, S. M., TULLER, H. L. Ultrasensitive chemiresistors based on electrospun TiO_2 nanofibers. *Nano Letters*, 2006. Vol. 6.9, p. 2009–2013.

[52] SAHAY, R., KUMAR, P. S., ARAVINDAN, V., SUNDARAMURTHY, J., LING, W. C., MHAISALKAR, S. G., RAMAKRISHNA, S., MADHAVI, S. High aspect ratio electrospun CuO nanofibers as anode material for lithium-ion batteries with superior cycleability. *The Journal of Physical Chemistry C*, 2012. Vol. 116.34, p. 18087–18092.

[53] BOGNITZKI, M., CZADO, W., FRESE. T., SCHAPER, A., HELLWIG, M., STEINHART, M., GREINER, A., WENDORFF, J. H. Nanostructured fibers via electrospinning. *Advanced Materials*, 2001. Vol. 13, p. 70–72.

[54] PANDA, P. K., RAMAKRISHNA, S. Electrospinning of alumina nanofibers using different precursors. *Journal of materials science*, 2007. Vol. 42.6, p. 2189–2193.

[55] WANG, X., DING, B., YU, J., WANG, M. Engineering biomimetic superhydrophobic surfaces of electrospun nanomaterials. *Nano today*, 2011. Vol. 6.5, p. 510–530.

[56] YOON, Y. L., MOON, H. S., LYOO, W. S., LEE, T. S., PARK, W. H. Superhydrophobicity of PHBV fibrous surface with bead-on-string structure. *Journal of colloid and interface science*, 2008. Vol. 320.1, p. 91–95.

[57] LI, L., JIANG, Z., LI, M., LI, R., FANG, T. Hierarchically structured PMMA fibers fabricated by electrospinning. *RSC Advances*, 2014. Vol. 4.95, p. 52973–52985.

[58] LUBASOVA, D., MARTINOVA, L., MAREKOVA, D., KOSTECKA, P. Cell growth on porous and non-porous polycaprolactone nanofibers. In: *Proceedings of the International Conference on Nano Technology (NANOCON'10)*. 2010.

[59] GREINER, A., WENDORFF, J. H. Electrospinning: a fascinating method for the preparation of ultrathin fibers. *Angewandte Chemie International Edition*. 2010. Vol. 46, p. 5670–5703.

[60] KALINOVA, K. Nanofibrous resonant membrane for acoustic applications. *Journal of Nanomaterials*, 2011.

[61] *Application areas.* [online]. [Accessed 3 January 2017]. Available from: http://www.elmarco.com/application-areas/medicine/

[62] MA, M., GUPTA, M., LI, Z., ZHAI, L., GLEASON, K. K., COHER, R. E., RUBNER, M. F. Decorated electrospun fibers exhibiting superhydrophobicity. *Advanced Materials*, 2007. Vol. 19, p. 255–259.

[63] XU, H., LI, H., CHANG, J. Controlled drug release from a polymer matrix by patterned electrospun nanofibers with controllable hydrophobicity. *Journal of Materials Chemistry B*, 2013. Vol. 33, p. 4182–4188.

[64] MENG, L. Y., PARK, S. J. Superhydrophobic carbon-based materials: a review of synthesis, structure, and applications. *Carbon Lett*, 2014. Vol. 15, p. 89–104.

[65] KANG, M., JUNG, R., KIM, H. S., JIN, H. J. Preparation of superhydrophobic polystyrene membranes by electrospinning. *Colloids and Surfaces A: Physicochemical and Engineering Aspects*, 2008. Vol. 313, p. 411–414.

[66] BACHMANN, J., MARMUR, A., DEURER, M. Soil hydrophobicity. *Encyclopedia of soil science, (2nd ed.) Abingdon (UK): Taylor and Francis,* 2006, Vol. 10, p. 1626–1629.

[67] ZHANG, X., SHI, F., NIU, J., JIANG, Y., WANG, Z. Superhydrophobic surfaces: from structural control to functional application. *Journal of Materials Chemistry*, 2008. Vol. 18, p. 621–633.

[68] *Sessile drop method.* [online]. [Accessed 28 January 2017]. Available from: http://membranes.edu.au/wiki/index.php/Sessile_Drop_Method

[69] TUPY, M., MERINSKA, D., SVOBODA, P., ZVONICEK, J. Influence of water and magnesium ion on the optical properties in various plasticized poly (vinyl butyral) sheets. *Journal of applied polymer science*, 2010. Vol. 118.4, p. 2100–2108.

[70] AMBROSIO, J. D., LUCAS, A. A., OTAGURO, H., COSTA, L. C. Preparation and characterization of poly (vinyl butyral)-leather fiber composites. *Polymer Composites*, 2011. Vol. 32.5, p. 776–785.

[71] ZHOU, Z. M., DAVID, D. J., MACKNIGHT, W. J., KARASZ, F. E. Synthesis characterization and miscibility of polyvinyl butyrals of varying vinyl alcohol contents. *Turkish Journal of Chemistry*, 1997. Vol. 21.4, p. 229–238.

[72] MLEZIVA, J. *Polymery - výroba, struktura, vlastnosti a použití*. 1. vyd. Praha: Sobotáles, 1993, ISBN 80-901-5704-1.

[73] FRIED, J. R. *Polymer science and technology*. (2nd ed.) Upper Saddle River, NJ: Prentice Hall Professional Technical Reference, 2003. ISBN 0130181684.

[74] OLABISI, O., ADEWALE, K. *Handbook of thermoplastics* (2nd ed.), CRC Press, Taylor & Francis Group, USA, 2016.

[75] DHALIWAL, A. K., HAY, J. N. The characterization of polyvinyl butyral by thermal analysis. *Thermochimica Acta*, 2002. Vol. 391, p. 245–255.

[76] SONEGO, M., COSTA, L. C., AMBROSIO, J. D. Flexible thermoplastic composite of polyvinyl butyral (PVB) and waste of rigid polyurethane foam. *Polímeros*, 2015. Vol. 25.2, p. 175–180.

[77] QIU, Y. R., MATSUYAMA, H. Preparation and characterization of poly (vinyl butyral) hollow fiber membrane via thermally induced phase separation with diluent polyethylene glycol 200. *Desalination*, 2010. Vol. 257.1, p. 117–123.

[78] *Polyvinyl butyral.* [online]. [Accessed 11 November 2016]. Available from: http://www.kuraray.eu/fileadmin/Downloads/pvb/Mowital_pioloform_broschuere_2013_17042013_low_quality_secured.pdf

[79] *Electrical conductivity information sheet.* [online]. [Accessed 8 January 2017]. Available from: http://www.gbwaterwatch.org.au/resources/ID1297390048.pdf

[80] *Wilhelmy plate method.* [online]. [Accessed 9 January 2017]. Available from: https://www.kruss.de/services/education-theory/glossary/wilhelmy-plate-meth-od/?sourceid=chrome&sugexp=chrome%2Cmod&cHash=f0c9d97d6e25b1b4d2f6503c75d1195e

[81] *Sessile drop.* [online]. [Accessed 9 January 2017]. Available from: https://www.kruss.de/services/education-theory/glossary/sessile-drop/

[82] *Rheology of thermosets Part 2: Rheometers.* [online]. [Accessed 1 November 2016]. Available from: https://polymerinnovationblog.com/rheology-thermosets-part-2-rheometers

[83] *Electron microscope. Encyclopedia Britannica.* [online]. [Accessed 12 November 2016]. Available from: https://www.britannica.com/technology/electron-microscope

[84] VOHLIDAL, J., JULAK, A., STULIK, K. *Chemické a analytické tabulky.* Praha: Grada, 1999. ISBN 80-7169-855-5.

.

LIST OF ABBREVIATIONS

A	cross-section area [m^2]
E	cohesion energy [J]
ΔH	latent heat of vaporization [J]
L	wetted length [m]
l	distance between the electrodes [m]
M_w	weight average molecular weight [g/mol]
R	universal gas constant [$J \cdot K^{-1} \cdot mol^{-1}$]
R_e	resistance [Ω]
r	radius of the sphere
RH	relative humidity [%]
T	absolute temperature [K]
γ	surface tension [mN/m]
γ_{LG}	interfacial tension between the liquid and gas [mN/m]
γ_{SG}	interfacial tension between the solid and gas [mN/m]
γ_{SL}	interfacial tension between the solid and liquid [mN/m]
$\dot{\gamma}$	shear rate [s^{-1}]
δ	Hansen solubility parameter [$MPa^{1/2}$]
δ_d	dispersive component [$MPa^{1/2}$]
δ_h	hydrogen bonding component [$MPa^{1/2}$]
δ_p	polar force component [$MPa^{1/2}$]
η	dynamic viscosity [Pa·s]
η_0	viscosity of solvent [Pa·s]
η_1	viscosity of solution [Pa·s]
η_{rel}	relative viscosity [-]

θ	contact angle [°]
κ	specific conductance [S/m]
v	kinematic viscosity [mm^2/s]
ρ	density [kg/cm^3]
ρ_s	specific resistivity [$\Omega \cdot m$]
σ	shear stress [Pa]
DMF	*N*, *N*-dimethylformamide
DMSO	dimethylsulfoxide
EtOH	ethanol
HSP	Hansen solubility parameter
MC	methylene chloride
MetOH	methanol
PC	polycarbonate
PCL	polycaprolactone
PEO	polyethylene(oxide)
PLLA	poly-L-lactide
PMMA	poly(methyl) metacrylate
PS	polystyrene
PVA	polyvinylalcohol
PVAC	polyvinyl acetate
PVB	polyvinylbutyral
SEM	scanning electron microscope
THF	tetrahydrofuran

LIST OF FIGURES

LIST OF TABLES